



UNIVERSITÉ DE NEUCHÂTEL  
INSTITUT DE PHYSIQUE

1011

# Etude dynamique de transitions de phase dans un réseau de jonctions Josephson

Forme réduite de la thèse présentée par Philippe Lerch  
pour l'obtention du grade de *dr è sciences*, 18 novembre 1987

jury composé de MM:  
Prof. Piero Martinoli (directeur de thèse)  
Prof. Hans Beck  
Prof. Bernard Pannetier (Grenoble)

1101

# IMPRIMATUR POUR LA THÈSE

Etude dynamique de transitions de phase  
dans un réseau de jonctions Josephson

de Monsieur Philippe Lerch

UNIVERSITÉ DE NEUCHÂTEL

FACULTÉ DES SCIENCES

La Faculté des sciences de l'Université de Neuchâtel,  
sur le rapport des membres du jury,

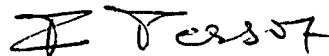
Messieurs P. Martinoli, H. Beck et

B. Pannetier (Grenoble)

autorise l'impression de la présente thèse.

Neuchâtel, le 16 novembre 1987

Le doyen:



F. Persoz

## Liste de publications

AC quantum interference in a 2D array of superconducting weak links, Ch. Leemann, Ph. Lerch and P. Martinoli, *Physica* 126, 475 (1984).

Dynamic conductance of a 2D array of Josephson junctions, Ch. Leemann, Ph. Lerch, G.A. Racine, A. Strupler and P. Martinoli, in *SQUID 1985*, edited by H.D. Hahlborn and H. Lübbig, 1065 (W. de Gruyter 1985).

Vortex dynamics and phase transition in a 2D array of Josephson junctions, Ch. Leemann, Ph. Lerch, G.A. Racine and P. Martinoli, *Phys. Rev. Lett.* 56, 1291 (1986).

The Kosterlitz and Thouless phase transition in Josephson junction array, Ch. Leemann, Ph. Lerch, R. Théron and P. Martinoli, *Helvetica Physica Acta* 60, 128 (1987).

Vortex dynamics in 2D arrays of superconducting weak links, P. Martinoli, Ch. Leemann and Ph. Lerch, in *Nonlinearity in Condensed Matter* edited by A.R. Bishop, D.K. Campbell, P. Kumar and S.E. Trullinger, 361, Springer Serie in Solid State Science 69 (Springer-Verlag Berlin 1987).

Dynamic conductance of a 2D array of Josephson junctions, Ph. Lerch, R. Théron, Ch. Leemann and P. Martinoli, *IEEE Trans. MAG-23*, 1126 (1987).

Arrays of Josephson junctions : Model systems for two-dimensional physics, P. Martinoli, Ph. Lerch, Ch. Leemann and H. Beck, Proc. 18th Int. Conf. on Low Temperature Physics, Kyoto, 1987, in the Japanese Journal of Applied Physics 26, Supplement 26-3 (1987).

Le texte intégral de la thèse intitulée " Etude dynamique de transitions de phase dans un réseau de jonctions Josephson " est déposé à l'Institut de physique de l'Université de Neuchâtel, Rue A.L. Breguet 1, 2000 Neuchâtel, CH.

AC QUANTUM INTERFERENCE IN A TWO-DIMENSIONAL ARRAY OF SUPERCONDUCTING WEAK LINKS

Ch. LEEMANN, Ph. LERCH and P. MARTINOLI

Institut de Physique, Université de Neuchâtel, CH-2000 Neuchâtel, Switzerland

The observation of quantum interference transitions in the dynamic resistance of a large two-dimensional array of proximity-effect junctions driven by superposed dc- and rf-currents is reported. It is shown that, under the synchronizing effect of the rf-field, the array behaves as a superposition of coherent quantum oscillators connected in series.

The resistive transition<sup>1-4</sup> and its magnetic field dependence<sup>5-8</sup> in regular two-dimensional (2D) arrays of superconducting weak links have recently received considerable attention. So far, however, the high-frequency behavior of large 2D arrays has not been investigated, the bulk of the experimental work in this field being restricted to 1D series arrays of weak links and/or to 2D arrays containing only a limited number of Josephson junctions<sup>9,10</sup>. Here we report the observation of quantum interference phenomena in a periodic 2D array of  $M \times N \approx 5 \times 10^5$  ( $M \times N$ ) Pb-Cu-Pb proximity-effect junctions exposed to electromagnetic radiation in the radio-frequency (rf) range. Our experiments show quite clearly that, under the synchronizing effect provided by the rf-field, the response of an array of  $M \times N$  superconducting weak links is equivalent to that of a "macroscopic" Josephson oscillator quantized in units of  $N(\hbar/2e)$  rather than  $(\hbar/2e)$ <sup>9-11</sup>.

The experiments were performed on an array consisting of rhombic 2200 Å thick Pb-islands forming a hexagonal Bravais lattice on a 1100 Å thick Cu-film. This pattern was obtained from a Pb-Cu proximity effect double layer using photolithography and sputteretching. The lattice parameter  $\alpha$  is 11.5 μm, the length of the Cu-bridges connecting adjacent Pb-rhombi roughly 2 μm. The resistance of the 2D array exhibits, with decreasing temperature, the two distinct transitions observed in similar systems by other groups<sup>1-3</sup>: the sharp BCS-transition of the Pb-islands at  $T_{CS} = 6.48$  K and the subsequent vortex-unbinding transition to zero resistance at an extrapolated  $T_C$  of about 0.9 K. Between  $T_C$  and the temperature  $T_C^0 \approx 1.5$  K corresponding to the onset of a state of phase-coherent Pb-islands, the resistance is found to be a periodic function of the transverse magnetic field  $B$ <sup>5-8</sup>, the period  $\Delta B = 2\phi_0/\alpha^2\sqrt{3} \approx 180$  mG corresponding to one flux quantum  $\phi_0$  per unit cell of the array.

To study the response of the array to an applied rf-field of angular frequency  $\omega$ , the sample was driven by superposed dc- and rf-currents and its dynamic resistance  $dV/dI$  measured as a function of the voltage  $V$  across the entire array. Derivative curves taken at differ-

ent frequencies are shown in Fig. 1. Pronounced structures reflecting the occurrence of quantum interference transitions show up at voltages  $V_n = n(N\hbar\omega/2e)$ , where  $n$  is an integer. From an analysis of data as those shown in Fig. 1, we deduce  $N = 725$ , a value corresponding almost exactly to the number of junctions crossed by the driving current as it flows through one "column" of the 2D array from one voltage probe to the other. Therefore, when exposed to rf-fields, a 2D array of  $M \times N$  weak links behaves as a coherent superposition of  $N$  elementary quantum oscillators connected in series<sup>9,11</sup>. The role

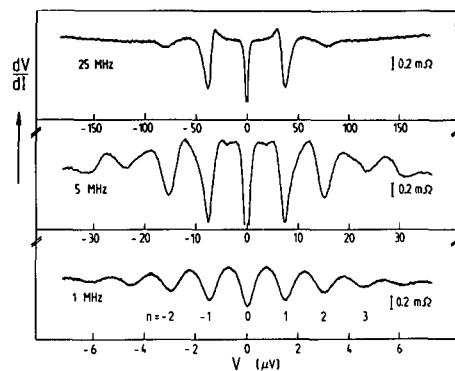


FIGURE 1  
 Dynamic resistance of a 2D array of Pb-Cu-Pb junctions exposed to rf-excitation.  $T = 1.20$  K.

of elementary oscillator is assigned to an individual "row" of  $M$  weak links perpendicular to the bias current. In a 2D array of nearly identical junctions the rf-field acts to synchronize the  $M$  links within an elementary oscillator at the Josephson frequency  $\omega_J = (2e/\hbar)V_J$ , where  $V_J$  is the voltage across the row, and to stimulate phase and frequency coherence among the  $N$  row-oscillators. This results in an array acting as

a macroscopic quantum oscillator obeying the voltage-frequency relation  $V = \Sigma V_J = (Nh/2e)\omega_J$ .

Interference transitions were observed up to  $n = 5$  and for frequencies ranging from 0.5 MHz up to 100 MHz, the upper frequency limit being determined by heating effects. It should be noticed that the collective quantum effects shown by the data of Fig. 1 were observed at a temperature  $T$  such that  $T_c < T < T_c^0$ , a result demonstrating the existence of long-range superconducting phase coherence in this temperature range.

The magnetic field dependence of the interference effect has also been investigated. Since resistance and critical current of the array are periodic in the magnetic flux  $\Phi$ , one expects the dynamic resistance of a quantum step to oscillate with  $B$ . This is shown in Fig. 2 for the  $N = 1$  interference transition. For comparison, the corresponding curve for the rf-unexcited array at zero dc-bias is also shown.

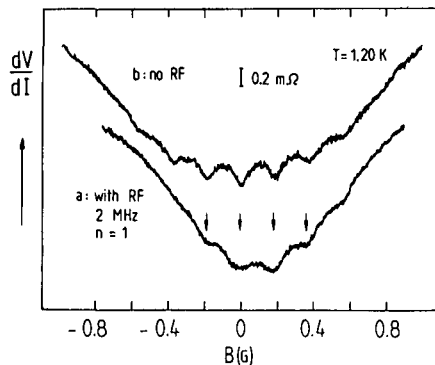


FIGURE 2

Dynamic resistance oscillations in a magnetic field: (a) with rf-excitation at the  $n=1$  quantum step; (b) without rf at zero dc-bias.

The question of whether coupling effects among the Josephson elements are strong enough to force the array into a self-synchronized superradiant state is still open at the moment and will be settled only by experiments conceived to detect the emitted radiation.

This work has been supported by the Swiss National Science Foundation.

#### REFERENCES

- (1) D.H. Sanchez and J.L. Berchier, *J. Low Temp. Phys.* **43**, 65 (1981).
- (2) D.J. Resnick, J.C. Garland, J.T. Boyd, S. Shoemaker and R.S. Newrock, *Phys. Rev. Lett.* **47**, 1542 (1981).
- (3) D.W. Abraham, C.J. Lobb, M. Tinkham and T.M. Klapwijk, *Phys. Rev. B* **26**, 5268 (1982).
- (4) R.F. Voss and R.A. Webb, *Phys. Rev. B* **25**, 3446 (1982).
- (5) R.A. Webb, R.F. Voss, G. Grinstein and P.M. Horn, *Phys. Rev. Lett.* **51**, 690 (1983).
- (6) B. Pannetier, J. Chaussy and R. Rammal, *J. Physique Lett.* **44**, L-853 (1983).
- (7) M. Tinkham, D.W. Abraham and C.J. Lobb, *Phys. Rev. B* **28**, 6578 (1983).
- (8) D. Kimhi, F. Leyvraz and D. Ariosa, *Phys. Rev. B* **29**, 1487 (1984).
- (9) T.D. Clark, *Phys. Rev. B* **8**, 137 (1973).
- (10) For a review see: J. Bindsvlev Hansen, PhD Thesis, University of Copenhagen (1981).
- (11) P. Martinoli, O. Daldini, Ch. Leemann and B. van den Brandt, *Phys. Rev. Lett.* **36**, 382 (1976).

## DYNAMIC CONDUCTANCE OF A TWO-DIMENSIONAL ARRAY OF JOSEPHSON JUNCTIONS

Ch. Leemann, Ph. Lerch, G.-A. Racine, A. Strupler and P. Martinoli

Institut de Physique, Université de Neuchâtel

CH - 2000 Neuchâtel, Switzerland

The complex conductance of large arrays of proximity effect junctions was measured. Close to the superconducting transition to zero dc resistance, we observe a peak in dissipation and a roll-off in the imaginary part of the conductance. The results are consistent with a description of vortex dynamics in terms of a dielectric constant containing contributions from vortex-antivortex pairs and free vortices.

A two-dimensional (2D) array of Josephson weak links is isomorphic to an XY-model with a temperature-dependent coupling energy  $E_J(T) = \hbar i_C(T)/2e$ , where  $i_C(T)$  is the critical current of an isolated junction of the array (1). According to the Kosterlitz-Thouless theory (2) of phase transitions in two dimensions, below a critical temperature  $T_C$  such a system is populated by bound pairs of vortices with opposite circulation resulting from thermal fluctuations in the phase of the order parameter. The resistive transition of the array at  $T = T_C$  is attributed to the dissociation of vortex-antivortex pairs, a process creating free vortex excitations which destroy the quasi long-range (or topological) order existing for  $T < T_C$ . Recent studies of the resistive transition and of the current-voltage characteristics of proximity-effect (3-5) and tunnel-junction (6) arrays were found to be consistent with calculations (7,8) based on the vortex-unbinding idea. Deeper insight into the physics of the vortex-unbinding transition is provided by experiments probing the unique features of the dynamic response of bound pairs and free vortices to a driving ac field as the temperature is swept across  $T_C$ . So far, such investigations have been restricted to superfluid helium films (9) and to thin superconducting layers (10). In this paper we report measurements of the complex sheet conductance  $G$  of an array of proximity-effect SNS junctions as a function of temperature and frequency. A peak in dissipation,  $\text{Re}(G)$ , and a roll-off in the imaginary part,  $\text{Im}(G)$ , of  $G$  are observed in the region of the transition and found to shift to higher temperatures with increasing driving angular frequency  $\omega$ , in qualitative agreement with dynamic extensions (11,12) of the Kosterlitz-Thouless theory.

The experiments were performed on arrays consisting of  $N \times N \approx 4 \times 10^5$  square 4000 Å-thick Pb-islands forming a square lattice (with lattice spacing  $a = 8 \mu\text{m}$ ) on a 2000 Å-thick Cu-film (13). The resistive transition of a typical array is shown in Fig. 1. There are two distinct transitions; the BCS transition of the individual lead islands at  $T_{CS}$  and, at a lower temperature labelled  $T_C$ , the transition to a superconducting state with long-range phase coherence. Between  $T_{CS}$  and  $T_C$  there is a region of expanding proximity effect in the Cu-bridges, which results in a slow decrease in resistance with temperature.

Measurements of the conductance  $G$  were made using a variation of the two-coil mutual inductance technique devised by Fiory and Hebard (14). Two concentric cylindrical coils were wound with  $20 \mu\text{m}$  diameter copper wire. The drive coil had a diameter of 4 mm and 20 turns evenly spaced over a distance of 4 mm. The inner receive coil had a diameter of 2 mm and consisted of two mutually compensating sections of 16 turns each. The coil assembly was immersed in stycast. After curing, the stycast was removed to within approximately  $10 \mu\text{m}$  of the beginning of the receive coil and the sample positioned directly under the coils. Residual dc magnetic fields perpendicular to the array were reduced to below 0.2 mG, a value corresponding to about 250 field-induced free vortices in the sample. Close to  $T_C$ , the rms voltage  $\delta V_\omega$  at the astatic-pair receive coil induced by

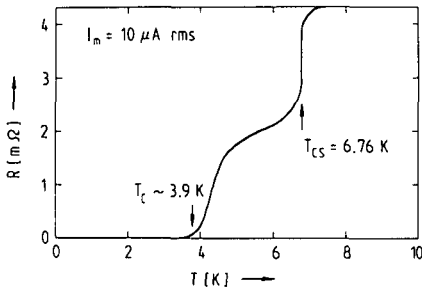


Fig. 1 : Temperature dependence of the dc resistance of a 2D array of Pb-Cu-Pb proximity effect junctions.  $T_{CS}$ : Transition of the lead islands.  $T_C$ : Vortex-unbinding transition.

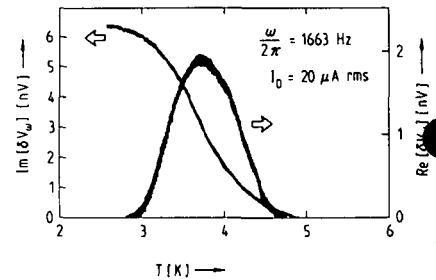


Fig. 2 : Temperature dependence of the receive coil signal  $\delta V_\omega$  proportional to the complex sheet conductance of the array at a frequency of 1663 Hz.

the currents flowing in the film is given by

$$\delta V_{\omega} \approx K\omega^2 I_{D\omega} G, \quad (1)$$

where  $I_{D\omega}$  is the rms amplitude of the excitation current in the drive coil and  $K$  depends only on the geometrical configuration of coils and sample. Equation (1) is valid in the weak screening limit defined by  $q\Lambda_R(T) \gg 1$ , where  $\Lambda_R(T)$  is the (renormalized) effective penetration depth and  $q^{-1}$  is a characteristic length related to the coil-sample geometry. For our system we find  $q\Lambda_R(T_C^-) \approx 22$ , where  $\Lambda_R(T_C^-)$  is the value of the penetration depth as one approaches  $T_C$  from below. It should be noticed, however, that  $\Lambda_R(T)$  is related to  $i_{CR}(T)$ , the (renormalized) critical current of a single junction, by (1) :

$$\Lambda_R(T) = \hbar / [e\mu_0 i_{CR}(T)]. \quad (2)$$

Thus, at low temperatures, where  $i_{CR}(T) \approx i_C(T)$  is large, the condition  $q\Lambda_R(T) \gg 1$  is no longer valid, and the response is determined by the geometrical inductance of the system.

Results for the real and imaginary parts of  $\delta V_{\omega}$  taken at a frequency of 1663 Hz are shown in Fig. 2 as a function of temperature. The data were obtained with  $I_{D\omega} = 20 \mu\text{A}$  rms, a current level producing an ac magnetic field of  $\sim 0.3$  mG at the center of the array. The phase of the phase-sensitive-detector was set to null the signal at low temperatures ( $T \ll T_C$ ). This phase setting was used for the measurement of  $\text{Re}(\delta V_{\omega})$ . With this choice we assume that the response of the array far below  $T_C$  is purely inductive. The evolution of the signals with varying frequency is shown in Figs. 3 and 4, where the voltage is normalized with respect to the driving angular frequency. Notice that the magnitude of  $\delta V_{\omega}/\omega$  is approximately independent of frequency. However, with increasing  $\omega$ , the peak in  $\text{Re}(\delta V_{\omega}/\omega)$  shifts to higher temperatures while the transition region broadens in both  $\text{Re}(\delta V_{\omega}/\omega)$  and  $\text{Im}(\delta V_{\omega}/\omega)$ .

In order to develop a qualitative understanding of the physics underlying the data shown in Figs. 3 and 4, we rely on the 2D Coulomb-gas analog of a vortex medium studied in Ref. 10. Combining this model with the static

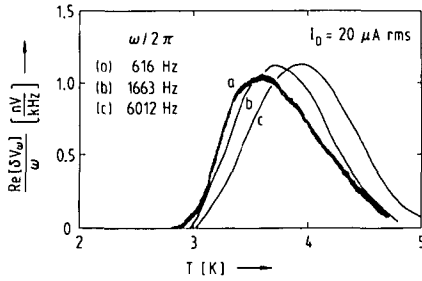


Fig. 3 : Real part of  $\delta V_{\omega}/\omega$  at three different driving frequencies.

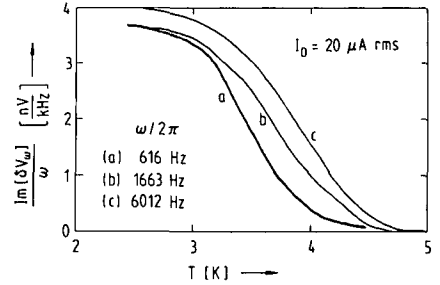


Fig. 4 : Imaginary part of  $\delta V_{\omega}/\omega$  at three different driving frequencies.

theory of the vortex-unbinding transition appropriate for arrays (1), it can be shown that the complex impedance  $Z(\omega, T) = G^{-1}(\omega, T)$  of an array with vortex excitations is given by

$$Z(\omega, T) = i\omega L_k \epsilon(\omega, T), \quad (3)$$

where  $L_k$  is the (unrenormalized) sheet kinetic inductance (1) and  $\epsilon(\omega, T)$  the complex dielectric constant of the vortex medium. From the above equations and the relation  $L_k = \mu_0 \Lambda / 2$ , it follows that close to  $T_C$  the vortex response, measured by  $\delta V_{\omega}/\omega$ , is proportional to  $i_c(T)/\epsilon(\omega, T)$ . The temperature dependence of  $i_c(T)$ , the critical current of a single junction in the absence of thermal fluctuations, has been inferred from critical current data of the array taken at low temperatures. Our measurements in the temperature regime  $1.2 \text{ K} < T < 3 \text{ K}$  can be accurately fitted to the Ginzburg-Landau expression

$$i_c(T) = i_c(0)(1 - T/T_{CS})^2 \exp(-L/\xi_N), \quad (4)$$

using a very reasonable normal metal coherence length  $\xi_N \approx 1400 \text{ \AA}$  at  $T_C$ . Here  $L \approx 1.8 \text{ \mu m}$  is the distance between adjacent lead islands. The monotonic temperature dependence of the critical current does not significantly influence the response of the array in the vicinity of  $T_C$ . The characteristic structures observed in  $\text{Re}(\delta V_{\omega}/\omega)$  and  $\text{Im}(\delta V_{\omega}/\omega)$  must therefore reflect the peculiar behavior of  $\epsilon^{-1}(\omega, T)$  in the transition re-

gion. To see this in more detail, we notice that  $\epsilon(\omega, T)$  is the sum of two contributions. The first contribution,  $\epsilon_b(\omega, T)$ , describes the response of bound vortex-antivortex pairs to the driving ac field.  $\epsilon_b(\omega, T)$  follows from the Kosterlitz scaling equations (9-12), in which the appropriate scale,  $\lambda_\omega$ , is set by the measuring frequency. It turns out that for an array of Josephson elements  $\lambda_\omega$  is given by

$$2\lambda_\omega = \ln[14r_n k_B T / (\phi_0^2 \omega)], \quad (5)$$

where  $r_n$  is the normal state resistance of a single junction. Taking  $r_n \approx 2.5 \text{ m}\Omega$ , a value deduced from a study of the dc resistance of the array, calculated values of  $\lambda_\omega$  for the data of Figs. 3 and 4 at  $T \approx 4 \text{ K}$  are, for increasing  $\omega$ , 2.4, 1.9 and 1.2 (the maximum scale,  $\ln N$ , is 6.4). These small scales point out the intrinsic difficulty one is faced with, when probing vortex dynamics in low resistance arrays using an inductive method. The second contribution to the dielectric constant,  $\epsilon_f(\omega, T) = \sigma_V(T) / (i\epsilon_0 \omega)$ , is associated with the plasma of free vortices above  $T_C$ . The free-vortex conductivity  $\sigma_V(T)$  is easily deduced from the theoretical work of Lobb et al (1) and can be written in the form

$$\sigma_V(T) = (2e\epsilon_0/\hbar)[a/\xi_+(T)]^2 i_C(T)r_n, \quad (6)$$

where  $\xi_+(T)$  is the vortex correlation length for  $T > T_C$  (2). The crossover from a response dominated by bound vortex pairs to one determined by a plasma of free vortex excitations occurs at a frequency dependent temperature  $T_\omega$  defined by  $\lambda_\omega = \ln[\xi_+(T_\omega)/a]$ . Calculations of  $\epsilon^{-1}(\omega, T)$  based on this simple model reveal the presence of a peak in  $\text{Re}(\epsilon^{-1})$  and a rolloff in  $\text{Im}(\epsilon^{-1})$  in the neighbourhood of  $T_\omega$ , in qualitative agreement with our experimental observations. A detailed quantitative comparison between the dynamic theory for the Kosterlitz-Thouless transition applicable to arrays and our measurements is in preparation and will be published elsewhere.

This work was supported by the Swiss National Science Foundation.

References :

- ( 1 ) C.J. Lobb, D.W. Abraham and M. Tinkham, Phys. Rev. B 27, 150 (1983)
- ( 2 ) J.M. Kosterlitz and D. J. Thouless, J. Phys. C 6, 1181 (1973)
- ( 3 ) D.J. Resnick, J.C. Garland, J.T. Boyd, S. Shoemaker and R.S. Newrock, Phys. Rev. Lett. 47, 1542 (1981)
- ( 4 ) D.W. Abraham, C.J. Lobb, M. Tinkham and T.M. Klapwijk, Phys. Rev. B 26, 5268 (1982)
- ( 5 ) D. Kimhi, F. Leyvraz and D. Ariosa, Phys. Rev. B 29, 1487 (1984)
- ( 6 ) R.F. Voss and R.A. Webb, Phys. Rev. B 25, 3446 (1982)
- ( 7 ) B.I. Halperin and D. R. Nelson, J. Low Temp. Phys. 36, 599 (1979)
- ( 8 ) P. Minnhagen, Phys. Rev. B 23, 5745 (1981); 24, 6758 (1981); 27, 2807 (1983)
- ( 9 ) D.J. Bishop and J.D. Reppy, Phys. Rev. Lett. 40, 1727 (1978); Phys. Rev. B 22, 5171 (1980)
- (10) A.F. Hebard and A.T. Fiory, Phys. Rev. Lett. 44, 291 (1980); Physica 109 & 110, 1637 (1982)
- (11) V. Ambegaokar, B.I. Halperin, D.R. Nelson and E.D. Siggia, Phys. Rev. Lett. 40, 783 (1978); Phys. Rev. B 21, 1806 (1980)
- (12) S.R. Shenoy, in Proc. of the 17th Int. Conf. on Low Temp. Phys. LT17, edited by U. Eckern, A. Schmid, W. Weber and H. Wühl (North-Holland, Amsterdam, 1984), p. 921
- (13) Ch. Leemann, Ph. Lerch and P. Martinoli, Physica 126B, 475 (1984)
- (14) A.T. Fiory and A.F. Hebard, AIP Conf. Proc. 58, 293 (1980)

## Vortex Dynamics and Phase Transitions in a Two-Dimensional Array of Josephson Junctions

Ch. Leemann, Ph. Lérch, G.-A. Racine, and P. Martinoli

*Institut de Physique, Université de Neuchâtel, CH-2000 Neuchâtel, Switzerland*

(Received 8 November 1985)

The ac response of large two-dimensional arrays of proximity-effect Josephson junctions to an oscillating driving field has been studied as a function of temperature, applied transverse magnetic field, and frequency. For an integer number of flux quanta per unit cell, a peak in dissipation and a drop in superfluid density are observed near the superconducting transition of the array. These features as well as their frequency dependence provide clear evidence for the vortex-unbinding transition predicted by the Kosterlitz-Thouless theory.

PACS numbers: 74.50.+r, 74.40.+k

This Letter reports a study of vortex dynamics in two-dimensional (2D) square arrays of Josephson junctions exposed to a transverse magnetic field  $\mathbf{B}$ . In the experiments described below, the complex ac response of vortex excitations to a driving oscillating field is inferred from measurements of the screening properties of the array performed with a two-coil mutual-inductance technique.<sup>1</sup> For an integer number of flux quanta per unit cell of the array we observe a peak in dissipation (as measured by the real part of the response) and a drop in superfluid density (as measured by the imaginary part of the response) in the vicinity of the superconducting transition of the array. The shapes of these structures, which are similar to those observed at the superfluid transition of 2D superfluid helium films<sup>2</sup> and of uniform 2D superconductors,<sup>1</sup> as well as their frequency dependence, provide clear evidence for the existence of a phase transition of the type predicted by the Kosterlitz-Thouless (KT) theory<sup>3</sup> and by its extensions<sup>4,5</sup> to finite frequencies.

In zero magnetic field a 2D array of identical Josephson junctions is isomorphic to an XY model with a temperature-dependent coupling energy  $E_J(T) = \hbar i_c(T)/2e$ , where  $i_c(T)$  is the critical current of an isolated junction of the array in the absence of thermal fluctuations.<sup>6</sup> According to the KT theory,<sup>3</sup> below a critical temperature  $T_c$  such a system is populated by bound pairs of vortices with opposite circulation resulting from 2D fluctuations in the phase of the order parameter. The phase transition of the system at  $T = T_c$  is attributed to the unbinding of vortex-antivortex pairs, a process creating free vortices which destroy the quasi long-range (or topological) order existing below  $T_c$ . Studies of the resistive transition and of the current-voltage characteristics of 2D arrays<sup>7-11</sup> were found to be consistent with the vortex-unbinding idea.

The physics of arrays of weak links exposed to a transverse  $\mathbf{B}$  field is more complex and only partially understood at present. The interaction of the field-

induced vortices with the pinning potential provided by the periodic structure of the array creates new and interesting phenomena which are most simply described by uniformly frustrated 2D lattice spin models,<sup>12-15</sup> the degree of frustration being controlled by the ratio  $f = \phi/\phi_0$ , where  $\phi = Ba^2$  is the magnetic flux threading a unit cell of the array ( $a$  is the lattice spacing) and  $\phi_0 = hc/2e$  the superconducting flux quantum. The frustration parameter  $f$  determines the ground-state configuration of the vortex lattice and, in addition, has a profound effect on the nature of the phase transition at  $T_c(f)$ . As  $f$  changes, the array is driven through a sequence of pinned commensurate (C) vortex phases and "floating" incommensurate (I) vortex phases. As a consequence, critical currents and resistance show a complex periodic dependence on  $f$ ,<sup>9-11,16,17</sup> similar to that observed earlier in other modulated superconducting structures.<sup>18,19</sup>

In order to explore the nature of the phase transition at  $T_c(f)$ , we have studied the dynamics of vortices in an array of proximity-effect Pb/Cu/Pb junctions using a modified version of the two-coil technique devised by Fiory and Hebard.<sup>1,20</sup> The experiments were performed on arrays consisting of  $N \times N \approx 5 \times 10^5$  square 4000-Å-thick Pb islands forming a square lattice with  $a = 8 \mu\text{m}$  on a 2000-Å-thick Cu film, the length  $L$  of the Cu bridges connecting adjacent Pb islands being of the order of  $1.7 \mu\text{m}$ . The zero-field dc resistance of the array shows, with decreasing temperature, the two distinct transitions observed in similar systems by other groups<sup>7-9</sup>: the sharp Bardeen-Cooper-Schrieffer transition of the individual Pb islands at  $T_{cs} = 7 \text{ K}$  and the subsequent transitions to the superconducting state at  $T_c \approx 3.4 \text{ K}$ . For the ac measurements the array was positioned directly under a system of coaxial cylindrical coils consisting of an external driving coil and an inner astatic-pair receiving coil. An ac current of amplitude  $I_{D\omega} = 35 \mu\text{A}$  rms and angular frequency  $\omega$  (varying from  $\sim 6 \times 10^2 \text{ s}^{-1}$  up to  $\sim 6 \times 10^4 \text{ s}^{-1}$ ) was applied to the driving coil and the signal voltage,  $\delta V_\omega$ , at the receiving coil due merely to the screening

currents flowing in the array was phase-sensitively detected.

Real and imaginary parts of  $\delta V_\omega$  measured at 4.033 kHz as a function of  $f$  are shown in Fig. 1 for different temperatures. Prominent structures emerge in both the dissipative [ $\text{Re}(\delta V_\omega)$ ] and inductive [ $\text{Im}(\delta V_\omega)$ ] components of  $\delta V_\omega$  in correspondence to C-vortex phases defined by integer ( $f=p$ ) and half-integer ( $f=p/2$ ) values of  $f$ . Structures at  $f=p/3$  are also clearly resolved in most of the data shown in Fig. 1. A detailed interpretation of the array response as a function of driving frequency, frustration, and temperature requires a theory describing the dynamics of field-induced vortices and of thermally generated topological excitations (vortices, dislocations, domain walls) in a periodic force field. Such a theory is not available so far. However, some of the essential features of  $\delta V_\omega(f, T)$  can be understood in terms of periodic vortex pinning and of the unique dynamic response of thermally excited vortices.

At low temperatures ( $T \ll T_c$ ), where the influence of topological excitations is negligible, structures in  $\delta V_\omega(f)$  at rational ( $f=p/q$ ) values of  $f$  reflect the drastic change in pinning occurring at a CI transition. In a low-order (small  $q$ ) C phase the mobility of the field-induced vortices is considerably reduced by the periodic pinning potential provided by the array, while the vortex lattice can slide freely in an I phase.<sup>18</sup> As a consequence, there is a marked reduction of dissipation in a low-order C phase, a process resulting in the periodic sequence of dips one observes in the  $\text{Re}[\delta V_\omega(f)]$  signals of Fig. 1(a) at low temperatures. On the other hand, since pinning is important in low-order C phases, considerable lag in response is expect-

ed for such vortex configurations. This is, of course, the mechanism responsible for the commensurate peaks occurring in the inductive component of  $\delta V_\omega(f)$  shown in Fig. 1(b).

As the temperature rises and approaches  $T_c$ , the low-temperature commensurate dips in  $\text{Re}[\delta V_\omega(f)]$  progressively transform into peaks which finally vanish above  $T_c$  [Fig. 1(a)]. Simultaneously, a rapid degradation of the commensurate peaks in  $\text{Im}[\delta V_\omega(f)]$  is observed in the critical region [Fig. 1(b)]. The evolution of the commensurate structures in both  $\text{Re}[\delta V_\omega(f)]$  and  $\text{Im}[\delta V_\omega(f)]$  suggests the presence of thermally activated defects<sup>11</sup> which, on account of their high mobility, generate additional dissipation and reduce the lag in response in a C phase. In the following we shall show that for integer  $f$  the dynamics of these defects has features allowing their unambiguous identification as the vortex excitations of the KT theory. To see this, we first consider the case  $f=0$  which is comparatively simpler. As for uniform thin-film superconductors,<sup>1</sup> the complex sheet impedance,  $Z_\square$ , of the array can be written in the form  $Z_\square(\omega, T) = i\omega L_{k\square}(T) \times \epsilon(\omega, T)$ , where  $L_{k\square}(T) = \hbar/2ei_c(T)$  is the bare sheet kinetic inductance of the array and  $\epsilon(\omega, T)$  is the complex vortex dielectric constant which renormalizes the bare superfluid density  $n^*(T) = m^*i_c(T)/2e\hbar$ .<sup>6</sup> In a 2D Coulomb-gas analog,  $\epsilon(\omega, T)$  is the sum of contributions from vortex-antivortex dipoles and free vortex charges.<sup>4</sup> In writing the above expression for  $Z_\square$  we have assumed that normal currents do not appreciably contribute to the total current flowing in the array, a condition satisfied if  $\omega L_{k\square} \ll r_n$ , where  $r_n$  is the normal-state resistance of an individual junction. Then, in the weak-screening limit<sup>20</sup> appropriate to discussion of our experiments in the critical region,<sup>21</sup> the signal voltage  $\delta V_\omega(T)$  turns out to be proportional to  $Z_\square^{-1}(\omega, T)$  and can be written in the form<sup>20</sup>

$$\delta V_\omega(T) = Ci\omega I_D \omega i_c(T) / \epsilon(\omega, T), \quad (1)$$

where  $C$  is a constant depending on the sample-coil geometrical configuration whose numerical value,  $C \approx 0.74 \text{ V s/A}^2$ , was deduced by the study of the frequency dependence of the jump in  $\text{Re}[\delta V_\omega(T)]$  at  $T_{cs}$ . Since the monotonic temperature dependence of  $i_c(T)$  does not significantly affect the response of the array in the vicinity of  $T_c$ , the behavior of  $\delta V_\omega(T)$  in the transition region will be mostly determined by  $\epsilon(\omega, T)$ . This is quite clearly demonstrated by the  $\delta V_\omega(T)$  signals for  $f=0$  shown in Fig. 2, where the peak in dissipation and the drop in superfluid density reflect the fundamental features of  $\epsilon^{-1}(\omega, T)$  predicted by dynamical extensions<sup>4,5</sup> of the KT theory.

Since the Hamiltonian of the system is periodic in  $f$  with period 1, the superconducting transition of the array is expected to be KT type also for  $f=p \neq 0$ . In this case the thermally activated defects are positive and

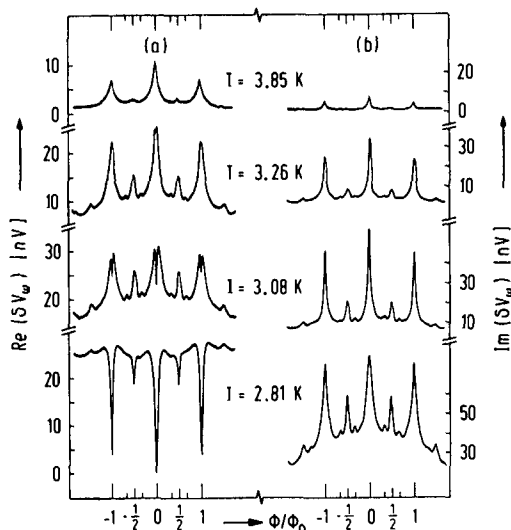


FIG. 1. (a) Real and (b) imaginary parts of the ac response at 4.033 kHz of a 2D array of proximity-effect Josephson junctions as a function of the frustration parameter  $f = \phi/\phi_0$ .

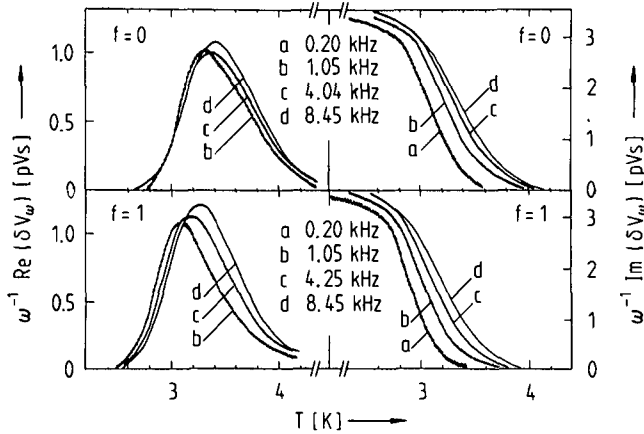


FIG. 2. Temperature dependence of the normalized complex ac response of the 2D array of Fig. 1 measured at different frequencies for  $f=0$  and  $f=1$ . Signal voltages are normalized with respect to angular frequency.

negative vacancies<sup>11</sup> associated, respectively, with  $p-1$  and  $p+1$  quantized vortices per unit cell. These vacancies of opposite sign can be viewed as free-moving vortex-antivortex excitations immersed in a pinned commensurate background of field-induced vortices with  $p$  flux quanta per unit cell. According to this picture, the response  $\delta V_\omega(T)$  for  $f=p \neq 0$  should be similar to that for  $f=0$ , a conjecture confirmed by the experimental results for  $f=1$  shown in Fig. 2. When compared with the case  $f=0$ , however, the transition is seen to occur at a lower temperature. This is easily understood if one realizes that the finite size of the junctions makes  $i_c$  field dependent. More precisely, as demonstrated by the parabolic envelope characterizing most of the signals of Fig. 1,  $i_c(T, f)$  is a quadratically decreasing function of  $f$  as long as  $(A/a^2)f \ll 1$ , where  $A$  is an effective area of the junctions. From the theoretical prediction<sup>6,10</sup>  $i_c(T_c(p), p)/T_c(p) \approx 4ek_B/\pi\hbar \approx 27$  nA/K, it then follows that the KT transition is pushed to lower temperatures by increasing  $p$ . It is also clear that Eq. (1) still describes the response in the more general case  $f=p$  provided one replaces  $i_c(T)$  by  $i_c(T, p)$ .

Further evidence for a vortex-unbinding transition at  $f=p$  is provided by a study of the frequency dependence of  $\delta V_\omega(T, p)$ . As shown in Fig. 2 by the data for  $f=0$  and  $f=1$ , the peak in  $\text{Re}[\delta V_\omega(T)]$  shifts to higher temperatures and the falloff of  $\text{Im}[\delta V_\omega(T)]$  broadens with increasing  $\omega$ . To discuss these results, we recall that the dynamical theories<sup>4,5</sup> introduce a vortex diffusion length  $r_\omega \approx (14D/\omega)^{1/2}$  determining the separation of those vortex pairs which dominate the response. The vortex diffusivity  $D$  is easily deduced from the analysis of the flux-flow regime in arrays by Lobb, Abraham, and Tinkham<sup>6</sup> and is found to be given by  $D = (c/\phi_0)^2 r_n a^2 k_B T$ . At finite frequencies the crossover in response due to the unbinding of

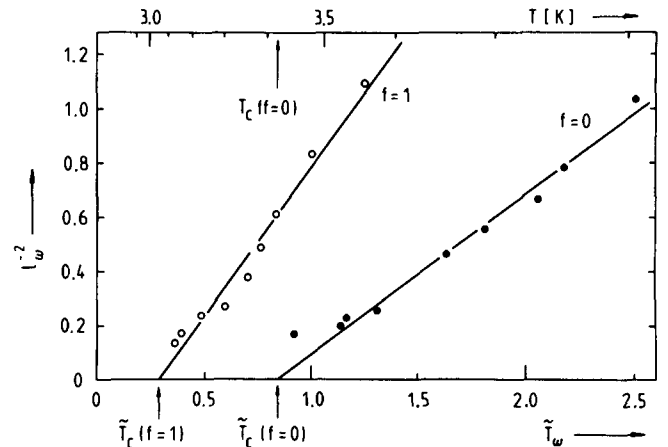


FIG. 3. Dependence of the scale parameter  $l_\omega \equiv \ln(r_\omega/a)$  on the dimensionless vortex-unbinding temperature  $\tilde{T}_\omega$ . Solid lines are fits according to Eq. (2). The upper axis is a real temperature scale for  $f=0$ .

bound vortex pairs into free vortices will be seen at a temperature  $T_\omega$  such that  $r_\omega = \xi_+(\tilde{T}_\omega)$ , where  $\xi_+(\tilde{T}) \approx a \exp\{b[\tilde{T} - \tilde{T}_c(p)]^{-1/2}\}$  is the correlation length of the array,  $\tilde{T} = 2ek_B T/\hbar i_c(T, p)$  a dimensionless temperature parameter, and  $b$  a nonuniversal constant of order unity.<sup>6</sup> Following Ref. 1, we define  $T_\omega$  by extrapolating to zero the steep portions of the  $\text{Im}[\delta V_\omega]$  vs  $T$  curves. We found that this procedure has the advantage of being largely independent of  $I_{D\omega}$ . Other definitions of  $T_\omega$ , for instance that proposed in Ref. 5 which identifies  $T_\omega$  as the temperature corresponding to the peak in  $\text{Re}[\delta V_\omega(T)]$ , were found to be very sensitive to  $I_{D\omega}$ , thereby showing the importance of nonlinear effects at finite driving currents.<sup>6-8</sup> If we introduce a scale parameter  $l_\omega \equiv \ln(r_\omega/a)$ , the condition  $r_\omega = \xi_+(\tilde{T}_\omega)$  can be written as

$$l_\omega^{-2} = b^{-2}[\tilde{T}_\omega - \tilde{T}_c(p)]. \quad (2)$$

In Fig. 3  $l_\omega^{-2}$  is plotted vs  $\tilde{T}_\omega$  for  $f=0$  and  $f=1$ . The scale  $l_\omega$  was calculated with  $r_n = 2.2$  m $\Omega$ , a value inferred from the sheet resistance of the array at  $T_{cs}^-$ . In this connection, we notice that, for a given  $\omega$ ,  $l_\omega$  in proximity-effect arrays is considerably smaller (in our experiments  $r_\omega/a$  ranges from  $\sim 3$  to  $\sim 13$ ) than in uniform 2D superconductors,<sup>1</sup> a fact accounting for the much broader transitions observed in our system. The  $i_c(T, p)$  curves needed to calculate  $\tilde{T}_\omega$  were obtained by the fitting of low-temperature  $i_c$  measurements by the expression<sup>22</sup>

$$i_c(T, p) = i_0(p)[1 - (T/T_{cs})]^2 \exp[-L/\xi_N(T)]$$

[using  $\xi_N(T_{cs}) = 850$  Å for the Cu coherence length,  $i_0(0) \approx 0.78$  A, and  $i_0(1) \approx 0.26$  A] and by extrapolation of the theoretical curves in the critical region. Good fits to Eq. (2) are obtained for  $b(f=0) = 1.29$  and  $b(f=1) = 0.95$  and lead to  $i_c(T_c(0), 0)/T_c(0)$

$= 49$  nA/K and  $i_c(T_c(1), 1)/T_c(1) = 143$  nA/K which, in turn, give  $T_c(0) = 3.43$  K and  $T_c(1) = 3.08$  K. In comparing these  $i_c/T_c$  ratios with the approximate theoretical prediction of 27 nA/K, it should be remembered that this value, resting on the assumption of an unrenormalized  $n^*(T, p)$ , underestimates  $i_c/T_c$ . Actually, static screening, described by  $\epsilon_c(p) = \epsilon(0, T_c(p))$ , renormalizes  $n^*(T, p)$  downwards, thereby leading to higher bare  $i_c/T_c$  ratios. For  $f=0$  we obtain  $\epsilon_c(0) = 1.81$ , a value in good agreement with an estimate for the XY model [ $\epsilon_c(0) \approx 1.75$ ] based on Monte Carlo calculations.<sup>23</sup> Because of additional dielectric screening provided by the commensurate vortex background,<sup>11</sup> renormalization effects should be more important for  $f=1$  than for  $f=0$  [ $\epsilon_c(1) > \epsilon_c(0)$ ]. This conjecture is consistent with the experimental observation of a larger  $i_c/T_c$  ratio for  $f=1$ , although additional screening alone seems to be insufficient to account for the large  $\epsilon_c$  value [ $\epsilon_c(1) = 5.3$ ] found in this case.

Finally, we briefly comment on the case  $f = \frac{1}{2}$ . We found that the response  $\delta V_\omega(T)$  looks quite similar to that for  $f=p$ , thereby suggesting a KT-type transition also for  $f=p/2$ . A study of the frequency dependence, however, did not confirm the exponential inverse square-root form for  $\xi_+(T)$ . The precise nature of the phase transition at  $T_c(p/2)$  (KT type or Ising type<sup>12</sup>) is therefore still unknown, a challenging problem which will deserve particular attention in our future work.

This work was supported by the Swiss National Science Foundation.

<sup>1</sup>A. F. Hebard and A. T. Fiory, Phys. Rev. Lett. **44**, 291 (1980), and Physica (Amsterdam) **109&110B+C**, 1637 (1982).

<sup>2</sup>D. J. Bishop and J. D. Reppy, Phys. Rev. Lett. **40**, 1727 (1978), and Phys. Rev. B **22**, 5171 (1980).

<sup>3</sup>J. M. Kosterlitz and D. J. Thouless, J. Phys. C **6**, 1181

(1973).

<sup>4</sup>V. Ambegaokar, B. I. Halperin, D. R. Nelson, and E. D. Siggia, Phys. Rev. Lett. **40**, 783 (1978), and Phys. Rev. B **21**, 1806 (1980).

<sup>5</sup>S. R. Shenoy, J. Phys. C **18**, 5163 (1985).

<sup>6</sup>C. J. Lobb, D. W. Abraham, and M. Tinkham, Phys. Rev. B **27**, 150 (1983).

<sup>7</sup>D. J. Resnick, J. C. Garland, J. T. Boyd, S. Shoemaker, and R. S. Newrock, Phys. Rev. Lett. **47**, 1542 (1981).

<sup>8</sup>D. W. Abraham, C. J. Lobb, M. Tinkham, and T. M. Klapwijk, Phys. Rev. B **26**, 5268 (1982).

<sup>9</sup>D. Kimhi, F. Leyvraz, and D. Ariosa, Phys. Rev. B **29**, 1487 (1984).

<sup>10</sup>R. F. Voss and R. A. Webb, Phys. Rev. B **25**, 3446 (1982).

<sup>11</sup>R. A. Webb, R. F. Voss, G. Grinstein, and P. M. Horn, Phys. Rev. Lett. **51**, 690 (1983).

<sup>12</sup>S. Teitel and C. Jayaprakash, Phys. Rev. B **27**, 598 (1983), and Phys. Rev. Lett. **51**, 1999 (1983).

<sup>13</sup>W. Y. Shih and D. Stroud, Phys. Rev. B **28**, 6575 (1983), and **30**, 6774 (1984), and **32**, 158 (1985).

<sup>14</sup>M. Y. Choi and S. Doniach, Phys. Rev. B **31**, 4516 (1985).

<sup>15</sup>T. C. Halsey, Phys. Rev. B **31**, 5728 (1985), and Phys. Rev. Lett. **55**, 1018 (1985).

<sup>16</sup>M. Tinkham, D. W. Abraham, and C. J. Lobb, Phys. Rev. B **28**, 6578 (1983).

<sup>17</sup>B. Pannetier, J. Chaussy, R. Rammal, and J. C. Villegier, Phys. Rev. Lett. **53**, 1845 (1984).

<sup>18</sup>O. Daldini, P. Martinoli, J. L. Olsen, and G. Berner, Phys. Rev. Lett. **32**, 218 (1974).

<sup>19</sup>A. T. Fiory, A. F. Hebard, and S. Somekh, Appl. Phys. Lett. **32**, 73 (1978).

<sup>20</sup>A. T. Fiory and A. F. Hebard, in *Inhomogeneous Superconductors—1979*, edited by D. U. Gubser, T. L. Francavilla, S. A. Wolf, and J. R. Leibowitz, AIP Conference Proceedings No. 58 (American Institute of Physics, New York, 1980), p. 293.

<sup>21</sup>At lower temperatures the weak-screening condition is no longer satisfied and Eq. (1) must be modified to account for the sample geometrical inductance (see Ref. 20).

<sup>22</sup>P. G. de Gennes, Rev. Mod. Phys. **36**, 225 (1964).

<sup>23</sup>J. Tobochnik and G. V. Chester, Phys. Rev. B **20**, 3761 (1979).

Reprint from

Springer Series in Solid-State Sciences, Volume 69

**Nonlinearity in Condensed Matter**

Editors: A. R. Bishop, D. K. Campbell, P. Kumar, and S. E. Trullinger

---

© Springer-Verlag Berlin Heidelberg 1987

Printed in Germany. Not for Sale.

Reprint only allowed with permission from Springer-Verlag



Springer-Verlag Berlin Heidelberg New York  
London Paris Tokyo

# Vortex Dynamics in Two-Dimensional Arrays of Superconducting Weak Links

*P. Martinoli, Ch. Leemann, and Ph. Lerch*

Institut de Physique, Université de Neuchâtel,  
CH-2000 Neuchâtel, Switzerland

## 1. Introduction

Ordering in a physical system strongly depends on its dimensionality  $d$  and on the number of degrees of freedom,  $n$ , of the quantity used to describe the order [1]. For instance, in a magnetic system  $n$  is the number of components of the spin ( $n = 1$  for the Ising model,  $n = 2$  for the XY model,  $n = 3$  for the Heisenberg model), while the description of the ordered phase of a superfluid in terms of a complex order parameter implies  $n = 2$ . In this context, two-dimensional systems ( $d = 2$ ) with  $n > 2$  hold, on account of the delicate problems they raise in connection with the possibility of a phase transition and with the nature of the ordered state that may occur at low temperatures [2-5], a very special position. Since the pioneering work of KOSTERLITZ and THOULESS [6] in the early 1970s, there has been considerable progress in the theoretical understanding of the critical behaviour of two-dimensional (2D) systems. It is now well established that topological excitations, such as vortices in 2D superfluids or dislocations in 2D solids, play a central role in critical phenomena occurring in these systems. For  $n = 2$  there is a sharp transition, triggered by the unbinding of pairs of topological excitations, from a low-temperature phase showing quasi long-range (or topological) order to a disordered phase at high temperatures, while for  $n > 2$  no phase transition at all occurs in two dimensions. Advances in material science, experimental techniques and numerical simulations have contributed to assess, in a variety of systems, the validity of the various theoretical ideas underlying the physics of phase transitions in two dimensions.

Recently, experiments on 2D regular arrays of Josephson junctions [7-14] and on 2D periodic superconducting networks [15,16] have stimulated a great deal of theoretical interest [17-28] in the critical behaviour of 2D lattice spin models. In zero magnetic field 2D periodic arrays of superconducting weak links are a physical realization of the XY model, a 2D lattice of planar ( $n = 2$ ) classical spins. For this system the Kosterlitz-Thouless (KT) theory [6] predicts, at a critical temperature  $T_C$ , a transition from a topologically ordered phase ( $T < T_C$ ) to a disordered phase ( $T > T_C$ ) driven by the unbinding of thermally excited vortex-antivortex pairs. The physics of 2D arrays of weak links exposed to a perpendicular magnetic field  $\vec{B}$  is more complex and only partially understood at present. The interaction of the vortices induced by the field with the pinning potential provided by the periodic structure of the array creates new and interesting phenomena which are most simply described by a uniformly frustrated XY model [17-25]. The degree of frustration is governed by the ratio  $f = \Phi/\Phi_0$ , where  $\Phi$  is the magnetic flux threading a unit cell of the array and  $\Phi_0 = hc/2e$  is the superconducting flux quantum. The frustration parameter  $f$  determines the ground-state ( $T = 0$ ) configuration of the vor-

tex lattice and, in addition, has a profound effect on the nature of the phase transition at  $T_c(f)$ . For instance, symmetry considerations for the fully frustrated ( $f = 1/2$ ) XY model [17,20-22] show that two kinds of topological excitations, vortices (point defects) and domain walls (line defects), are relevant in determining the critical behaviour of the array. As a consequence, one is faced with the possibility of two competing phase transitions, one driven by vortex unbinding (KT-like transition) the other by the proliferation of domain walls (Ising-like transition). The question of whether these two transitions are distinct or merge into a single transition belonging to a new universality class is presently a subject of theoretical speculations [17-25].

Studies of the resistive transition and of the current-voltage characteristics of 2D arrays in zero field ( $f = 0$ ) were found consistent with the vortex-unbinding idea [7,8,10-12]. Moreover, resistance and critical current measurements [9-12, 16, 17] show a complex periodic dependence on  $f$ , reflecting the fact that, by varying  $f$ , the array is driven through a periodic sequence of pinned commensurate vortex phases and "floating" incommensurate vortex phases. A somewhat similar behaviour was observed earlier in other periodic 2D superconducting structures [29, 30].

In a recent Letter [13] we reported a study of vortex dynamics in a 2D square array of proximity - effect coupled Josephson junctions. In those experiments the complex ac response of vortex excitations to a driving oscillating field was inferred from measurements of the screening properties of the array. For an integer number of flux quanta per unit cell a peak in dissipation and a drop in superfluid density were observed in the critical region. The shape of these structures, which are reminiscent of those observed at the superfluid transition of uniform 2D superconductors [31] and of 2D superfluid helium films [32], as well as their frequency dependence were found to agree with predictions of the KT theory [6] and of its extensions [33,34] to finite frequencies.

In this paper we give a fairly detailed account of vortex dynamics in 2D arrays of Josephson junctions. We shall mainly focus on the critical behaviour of the unfrustrated system, deferring the discussion of the effect of frustration on the nature of the phase transition at  $T_c(f)$  to a subsequent publication. Some qualitative aspects of the dynamics of field-induced vortices in commensurate and incommensurate vortex phases at low temperatures are also discussed.

## 2. Arrays in Zero Magnetic Field

Consider a 2D square lattice of superconducting islands connected by Josephson weak links. Only nearest-neighbour islands are assumed to interact with each other. The interaction energy  $E_{ij}$  of a pair of islands is the energy necessary to create a difference  $(\phi_j - \phi_i)$  in the phase of the superconducting order parameter between the nearest-neighbour lattice sites  $i$  and  $j$ . Using Josephson's fundamental equations,  $E_{ij}$  turns out to be given by :

$$E_{ij} = [\hbar i_c(T)/2e] [1 - \cos(\phi_j - \phi_i)] \quad , \quad (1)$$

where  $i_c(T)$  is the critical current of the (isolated) junction  $\langle ij \rangle$  in the absence of thermal fluctuations [35]. Summing over all nearest-neighbour pairs  $\langle ij \rangle$ , the Hamiltonian of the system will be :

$$H = [\hbar i_c(T)/2e] \sum_{\langle ij \rangle} [1 - \cos(\phi_j - \phi_i)] \quad . \quad (2)$$

If one identifies the phase variable  $\phi_i$  with the angle a planar ( $n = 2$ ) spin at the site  $i$  makes with a fixed arbitrary direction in the lattice plane, then Eq. (2) shows quite clearly that a 2D array of Josephson junctions is isomorphic to an XY model with a temperature-dependent coupling energy  $J = \hbar i_c(T)/2e$ . As a consequence, the statistical mechanics of the of the system is conveniently described in terms of a dimensionless temperature parameter  $T \equiv k_B T/J(T) = 2ek_B T/\hbar i_c(T)$  [35].

### 2.1 The Kosterlitz - Thouless Phase Transition

According to an important theorem due to MERMIN and WAGNER [4] and to HOHENBERG [5], a 2D array of weak links is precluded from developing, at finite temperatures, a state showing conventional long-range order in the phases  $\phi_i$  by spontaneously breaking a continuous symmetry, in this case a uniform global rotation of the  $\phi_i$ 's. However, calculations based on "spin-wave" excitations of the phase show that, at sufficiently low temperatures, the "spin-spin" correlation function decays algebraically with distance, a behaviour requiring some kind of phase transition to the high-temperature régime where the correlation function is expected to decay exponentially, as in a liquid. The nature of this novel phase transition was explained by KOSTERLITZ and THOULESS [6] with the introduction of vortices and antivortices as additional topological excitations resulting from 2D fluctuations in the phase of the order parameter.

According to the KT theory, for  $T < T_c$  the system is populated by bound pairs of vortices with opposite circulation. In an array the potential energy of a vortex-antivortex pair with cores separated by a distance  $r$  is given by [36] :

$$U(r) = [\hbar i_c(T)/2e] \ln(r/a) \quad , \quad (3)$$

where  $a$  is the lattice spacing. The logarithmic dependence of  $U(r)$  on  $r$  is valid as long as  $r$  is less than the effective penetration depth  $\Lambda(T) = (c\Phi_0/4\pi^2)/i_c(T)$  of the array [36]. It turns out, however, that, at  $T = T_c$ ,  $\Lambda(T_c)$  is approximately given by the relation  $\Lambda(T_c) T_c \approx 1.96$  cmK. It follows that for typical values of  $T_c$  (a few Kelvin)  $\Lambda(T_c)$  is a macroscopic length. Thus, in the interesting critical region the condition  $r < \Lambda$  is nearly satisfied even by the largest vortex pairs (for which  $r$  is of the order of the linear dimension,  $N_a$ , of the array) excited in a typical array ( $N_a \lesssim 1$  cm).

The above expression for  $U(r)$  shows that vortex excitations in a 2D array interact as electric charges in a 2D Coulomb gas. This analogy allows one to define a "vortex charge"  $q_v$  as follows :

$$2q_v^2/\lambda = \hbar i_c(T)/2e \quad , \quad (4)$$

where  $\lambda$  is the length of the vortex charge.

Below  $T_c$ , the array is in a superconducting state with quasi long-range (or topological) order in the phase of the order parameter. Thermally excited vortex-antivortex pairs, together with "spin wave" excitations, lead to an algebraically decaying correlation function of the form [6] :

$$\langle \exp[i\{\phi(\underline{R}) - \phi(\underline{0})\}] \rangle \sim R^{-\eta_R(T)}, \quad (5)$$

where the exponent  $\eta_R(T)$  is related to  $J_R$ , the coupling energy "renormalized" by the presence of bound vortex pairs (see below), by  $\eta_R(T) = k_B T / 2\pi J_R$ .

The phase transition of an infinite 2D array at  $T = T_C$  is triggered by the undinding of the vortex-antivortex pairs of largest separation ( $r \rightarrow \infty$ ). As the temperature increases above  $T_C$ , the unbinding mechanism progressively extends to pairs of smaller and smaller size, a process creating an increasing number of free vortices which destroy the topological order existing below  $T_C$ . In the disordered state above  $T_C$  short-range correlations in the phases  $\phi_i$  are described by [37] :

$$\langle \exp[i\{\phi(\underline{R}) - \phi(\underline{0})\}] \rangle \sim e^{-R/\xi_+(T)}, \quad (6)$$

where the correlation length  $\xi_+(T)$  has an unusual temperature dependence reflecting the very peculiar nature of the KT transition :

$$\xi_+(T) \approx a \exp[b(\tilde{T} - \tilde{T}_C)^{-1/2}], \quad (7)$$

where  $b$  is a non-universal constant of order unity. Physically,  $\xi_+(T)$  is a measure of the average distance between free vortices. Accordingly, the free-vortex areal density  $n_{f_0}$  is approximately given by  $n_{f_0} \approx \xi_+^{-2}(T)$ .

The potential energy (3) of a vortex-antivortex pair with separation  $r$  is reduced (or "renormalized") by the presence of intervening pairs of smaller size. Referring to the 2D Coulomb gas analogue, the resulting screened interaction between the members of a pair of size  $r$  is conveniently described in terms of a scale-dependent dielectric constant  $\epsilon(r)$  which increases with  $r$  and is such that  $\epsilon(a) = 1$ . The calculation of  $\epsilon(r)$  is based on the Kosterlitz scaling equations [36, 37], a set of coupled recursion relations for the reduced "spin-wave" stiffness constant  $K(r) = (J/k_B T) \epsilon^{-1}(r) = [\tilde{n}_C(T)/2ek_B T] \epsilon^{-1}(r)$  and the vortex thermal activity  $y(r)$ . An important prediction of the renormalized KT theory is that at  $T_C$  and for infinite scale ( $r \rightarrow \infty$ )  $K(\infty) \equiv K_R$  has the universal value  $2/\pi$ . For a 2D array of weak links the universal relation can be written in the form [35, 36] :

$$i_C(T_C)/\epsilon_C T_C = 8ek_B/h \approx 27 \text{ nA/K}, \quad (8)$$

where  $\epsilon_C$  is the value of  $\epsilon(r)$  at  $T_C$  and for  $r \rightarrow \infty$ . Since, at  $T_C$   $J_R = J/\epsilon_C$ , an alternative formulation of the KT universal result is that the exponent  $\eta_R(T)$  in Eq. (5) has the value  $1/4$  at the transition. The value of  $\epsilon_C$  depends on the parameters which determine the detailed form of the core potential,  $\mu(T)$ , of a vortex excitation, a quantity related to the vortex activity at the shortest scale  $r = a$  by  $y(a) \sim \exp[-\mu_C(T)/k_B T]$  [36]. For the XY model on a square lattice, KOSTERLITZ and THOULESS found  $\epsilon_C \approx 1.175$ , while from Monte Carlo calculations [38] one infers  $\epsilon_C \approx 1.75$ .

## 2.2. Vortex Dynamics

The dynamics of vortex excitations near the phase transition of 2D systems has unique features which, when seen in an appropriately conceived experiment, allow a crucial and detailed test of the KT theory [13, 31, 32].

The dynamical properties of the KT transition were studied by AMBEGAOKAR et al. [33] for 2D superfluids and, more recently, by SHENOY [34] for 2D arrays of Josephson junctions. In these models the response, near  $T_C$ , of bound vortex pairs and of free vortices to a driving oscillating field of angular frequency  $\omega$  is described in terms of a temperature and frequency-dependent complex dielectric constant  $\epsilon(T, \omega)$ . Carrying on the analogy with the 2D Coulomb gas,  $\epsilon(T, \omega)$  can be written as the sum of a contribution  $[\epsilon_b(T, \omega) - 1]$  due to the polarization of vortex-antivortex dipoles and of a "Drude term"  $\epsilon_f(T, \omega) = \{1 + [4\pi\sigma_v(T)/i\omega]\}$ , where  $\sigma_v(T)$  is the vortex conductivity, describing dynamical screening of the free-vortex plasma, i.e.:

$$\epsilon(T, \omega) = \epsilon_b(T, \omega) + [4\pi\sigma_v(T)/i\omega] \quad (9)$$

The motion of a bound vortex pair with separation  $r$  in response to the driving ac field is characterized by the time  $\tau(r) \sim r^2/D_v$  which governs its diffusive relaxation towards the equilibrium orientation ( $D_v$  is the vortex diffusivity). In the dynamical theories [33, 34] the bound-pair contribution  $\epsilon_b(T, \omega)$  in Eq. (9) is obtained from the scale-dependent dielectric constant  $\epsilon(r)$  introduced in Sec. 2.1 by integrating over a continuous distribution of relaxation times  $\tau(r)$ . This procedure singles out a characteristic scale, the vortex diffusion length

$$r_\omega \approx (14D_v/\omega)^{1/2} \quad (10)$$

which determines the separation of those vortex pairs which dominate the response. Then, an approximate calculation shows that  $\epsilon_b(T, \omega)$  is related to  $\epsilon(r_\omega)$  in the following way :

$$\text{Re } \epsilon_b(T, \omega) \approx \epsilon(r_\omega) \quad (11)$$

$$\text{Im } \epsilon_b(T, \omega) \approx (\pi/4) [r d\epsilon/dr]_r = r_\omega$$

Recalling that  $\xi_+(T)$  is a measure of the average distance between free vortices, the existence of a characteristic length scale  $r_\omega$  at finite frequencies indicates that there is a crossover in response due to the unbinding of bound vortex pairs with separation  $r_\omega$  into free vortices at a temperature  $T_\omega > T_C$  such that :

$$r_\omega \approx \xi_+(T_\omega) \quad (12)$$

This relation, together with Eqs.(7) and (10), shows that, by probing the system with increasing frequency, the vortex-unbinding transition should be seen to shift to higher temperatures.

Above  $T_C$ , the contribution of free vortices to  $\epsilon(T, \omega)$  can be easily estimated by writing the free-vortex conductivity  $\sigma_v(T)$ , in the spirit of the 2D Coulomb gas analogue, as  $\sigma_v(T) = q_v^2 n_f(T) \mu_v = (q_v^2/\ell) n_{f_\square}(T) \mu_v$ , where the vortex charge  $q_v$  is given by Eq.(4) and  $n_{f_\square} \approx \xi_+^{-2}(T)$  (see Sec. 2.1). The vortex mobility  $\mu_v$  can be easily expressed in terms of array parameters following the analysis of the flux-flow régime in arrays by LOBB et al.[35]. It turns out that, in the critical region,  $\mu_v$  can be written, to a very good approximation, as :

$$\mu_v \approx (c/\Phi_0)^2 a^2 r_n \quad (13)$$

where  $r_n$  is the normal-state resistance of an individual junction. Finally, using Eqs. (4) and (10), the vortex conductivity becomes :

$$\sigma_v(T) = (e/h) [a/\xi_+(T)]^2 i_c(T)r_n \quad , \quad (14)$$

an expression showing that  $\sigma_v$  is proportional to the fraction of area occupied by the vortex cores (of radius  $\sim a$ ) and to the  $i_c r_n$  - product of a single weak link. Notice that, using Eq. (13) and Einstein's relation  $D_v = \mu_v k_B T$ , the vortex diffusivity entering Eq. (10) can be expressed as  $D_v = (c/\Phi_0)^2 a^2 r_n k_B T$ .

In Sec. 4 it will be shown that, near the phase transition, the signal voltage  $\delta V_\omega(T)$  which measures the ac response of the array in our experiments is inversely proportional to  $\epsilon(T, \omega)$ . Calculations of  $\epsilon^{-1}(T, \omega)$  based on the previous discussion and on the Kosterlitz scaling equations show that, as  $T$  crosses  $T_\omega$  from below, there is a drop in  $\text{Re}(\epsilon^{-1})$ , while a peak emerges in  $\text{Im}(\epsilon^{-1})$ . The fall-off in  $\text{Re}(\epsilon^{-1})$  reflects the smooth drop in superfluid density one expects when vortex unbinding is probed at a finite scale  $r_\omega$  (a discontinuous jump occurs at infinite scale only). The peak in  $\text{Im}(\epsilon^{-1})$ , on the other hand, is a manifestation of the crossover from a bound-pair dominated dissipation [ $r_\omega < \xi_+(T)$ ] to a free-vortex - dominated dissipation [ $r_\omega > \xi_+(T)$ ].

### 3. Arrays in a Magnetic Field

Two-dimensional arrays of Josephson junctions exposed to a perpendicular magnetic field  $\vec{B}$  are isomorphic to a frustrated XY model with the Hamiltonian [17-20, 39] :

$$H = [\hbar i_c(T)/2e] \sum_{\langle ij \rangle} [1 - \cos(\phi_j - \phi_i - A_{ij})] \quad , \quad (15)$$

where  $A_{ij}$  is proportional to the line integral of the vector potential  $\vec{A}$  from the site  $i$  to the site  $j$  :  $A_{ij} = (2\pi/\Phi_0) \int_i^j \vec{A} \cdot d\vec{s}$ . In a square lattice each plaquette contains four weak links with a phase difference  $(\phi_j - \phi_i - A_{ij})$  across the link  $\langle ij \rangle$ . Then, the requirement that the phase of the superconducting wave function must change by an integral multiple of  $2\pi$  in going around a closed path implies [9, 17-20, 39] :

$$\sum_p (\phi_j - \phi_i - A_{ij}) = -2\pi f \pmod{2\pi} \quad , \quad (16)$$

where the sum is over the four links in the plaquette. If the transverse penetration depth is large compared to the sample size ( $\Lambda > Na$ ), screening currents are negligible and, as a consequence, the magnetic field penetrates the array uniformly. In this case  $f\Phi_0$  is constant throughout the array and equal to the magnetic flux,  $\Phi = Ba^2$ , threading a unit cell.

The Hamiltonian (15) is a periodic even function of  $f$  with period 1. As a consequence, we can restrict our attention to the interval  $0 < f < 1/2$ . While for an isolated plaquette the ground-state phase configuration is such that Eq. (16) is satisfied by taking  $(\phi_j - \phi_i - A_{ij}) = -(\pi/2)f$ , in an array frustration effects resulting from competing interactions with neighbouring cells make the determination of the ground state a difficult problem. For  $1/3 < f < 1/2$  an interesting quasi one-dimensional solution has been proposed by HALSEY [20]. For a square lattice the supercurrent dis-

tribution in the ground state consists of a sequence of "staircase" supercurrents generating a striped quasi 1D structure along a diagonal of the lattice. Staircase supercurrent patterns for  $f = 1/2$  and  $f = 1/3$  are shown in Fig. 1(a) along with the corresponding phase configurations. We refer to this description in terms of phases and currents as the "phase-current picture". The gauge-invariant phase differences  $(\phi_j - \phi_i - A_{ij})$  are identical for all links located on a given staircase. Therefore, magnitude and sign of the supercurrent are constant along the same staircase. As required by Kirchhoff's law, the supercurrent is conserved at each lattice site. Numerical calculations agree with the staircase model for  $1/3 < f < 1/2$ . For other values of  $f$ , no analytical solution exists so far and the ground state has been constructed by Monte Carlo and mean field methods [17, 18].

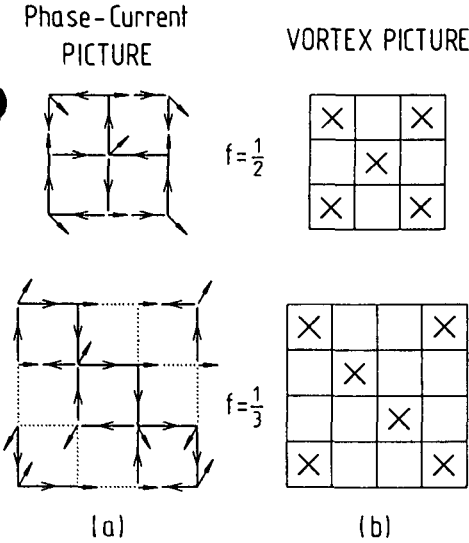


Fig. 1 Ground states of a 2D array for  $f = 1/2$  and  $f = 1/3$  (a) Staircase current patterns and phase configurations in the phase-current model. (b) Commensurate vortex phases in the vortex model.

An equivalent and, in several circumstances, useful way of describing ground states of a frustrated 2D array of weak links is provided by what we call the "vortex picture". In this model the ground state is determined by considering the interaction of the vortex lattice induced by the magnetic field with the pinning potential created by the periodic structure of the array. Since there are two competing periodicities, as  $f$  changes the array is driven through a sequence of commensurate (C) ( $f = p/q$  rational, where  $p$  and  $q$  are integers such that  $p/q$  is an irreducible fraction) and incommensurate (I) ( $f$  irrational) vortex phases, whose detailed structure can be found by mapping the Hamiltonian (15), via a Villain duality transformation [40], onto a lattice 2D Coulomb gas [17, 20]. C-vortex configurations for  $f = 1/2$  and  $f = 1/3$  are shown in Fig. 1 (b). The ground state of a C-phase is characterized by the formation of a superlattice with a  $(qa \times qa)$  unit cell.

At low temperatures [ $T \ll T_c(f)$ ], C-vortex phases are pinned by the periodic potential provided by the array. As a function of  $f = p/q$ , the pinning strength, as measured by the critical current,  $i_c(f=p/q)$ , of the array, has a strongly discontinuous upper bound  $\pi(e/\hbar) \epsilon(f=p/q) q^{-1}$ , where

$\epsilon(f=p/q)$  is the (non-monotonic) ground-state energy per junction [17]. In an I-phase, on the other hand, the vortex lattice can slide freely [ $\epsilon(f=p/q)/q=0$  for  $q \rightarrow \infty$ ]. Thus, in experiments probing vortex dynamics as a function of  $f$ , marked structures should appear in the complex ac response of an array in correspondence to low-order (small  $q$ ) C-phases. Such experiments will be discussed in some detail in Sec. 4.

Concerning the nature of the phase transition at  $T_c(f)$ , in this paper we restrict our discussion to the unfrustrated ( $f = p$ ) case. Since the Hamiltonian (15) is periodic in  $f$  with period 1, the superconducting transition of a 2D array of weak links is expected to be KT-like also for  $f = p \neq 0$ . In this case the thermally activated point defects are positive and negative vacancies associated, respectively, with  $(p - 1)$  and  $(p + 1)$  quantized vortices per unit cell. These vacancies of opposite sign can be viewed as free-moving vortex-antivortex excitations immersed in a pinned commensurate background of field-induced vortices with  $p$  flux quanta per unit cell [13].

#### 4. Experimental Results and Discussion

We have studied [13] the dynamics of vortices in 2D arrays of proximity-effect Pb/Cu/Pb junctions using a modified version of the two-coil technique devised by FIDRY and HEBARD [41]. The experiments reported here were performed on two arrays, A1 and A2, consisting of  $N \times N \approx 5 \times 10^5$  square Pb islands forming a square lattice with  $a = 8 \mu\text{m}$  on a Cu layer, the length  $L$  of the Cu bridges connecting adjacent Pb islands being of the order  $1.7 \mu\text{m}$ . A1 and A2 differ in the thicknesses of the superconducting islands and of the normal film, thereby having slightly different coupling energies. The zero-field dc resistance of both arrays shows, with decreasing temperature, the two distinct transitions observed in similar systems by other groups [7, 8, 10]. For the ac measurements the arrays were positioned directly under a system of coaxial cylindrical coils consisting of an external driving coil and an inner astatic-pair receiving coil [42]. An ac current of amplitude  $I_{D\omega}$  and angular frequency  $\omega$  was applied to the driving coil and the signal voltage,  $\delta V_\omega$ , at the receiving coil due merely to the screening currents flowing in the array was phase-sensitively detected. It turns out that, for our sample-coil geometrical configuration,  $\delta V_\omega$  is related to the complex sheet impedance,  $Z_\square$ , of the array by [41] :

$$\delta V_\omega = -\omega^2 I_{D\omega} Z_\square^{-1} \int_0^\infty e^{-x} f(x) [x + (H/\Lambda) (i\omega L_{K_\square}/Z_\square)]^{-1} dx, \quad (17)$$

where  $L_{K_\square}(T) = (2\pi/c^2)\Lambda(T) = \hbar/2e i_c(T)$  is the bare sheet kinetic inductance of the array,  $H$  the distance of the first (lowest) winding of the driving coil from the array ( $H \approx 0.3\text{mm}$ ) and  $f(x)$  an oscillating function of  $x$ , such that  $f(0) = 0$ , decaying as  $1/x^2$  at large  $x$  and depending only on the geometrical parameters of the coils.

If one assumes that normal currents do not appreciably contribute to the total current flowing in the array, i.e. if  $\omega \ll r_n/L_{K_\square}$ , then for  $f = 0$   $Z_\square(T, \omega)$  can be written in the form [13, 31] :

$$Z_\square(T, \omega) = i\omega L_{K_\square}(T) \epsilon(T, \omega), \quad (18)$$

an expression which explicitly shows that vortex excitations described by  $\epsilon(T, \omega)$  [Eq. (9)] renormalize the bare areal superfluid density

$n_{\alpha}^*(T) = m^*/4e^2 L_{K_{\alpha}}(T)$  downwards. In our experiments  $H$  is much smaller than  $\Lambda$  in the transition region. Accordingly, near  $T_C$  the term proportional to  $(H/\Lambda)$  in Eq. (17) can be ignored and  $\delta V_{\omega}$  becomes, using Eq. (18) :

$$\delta V_{\omega} \approx C i_{\omega} I_{D_{\omega}} i_c(T) / \epsilon(T, \omega) \quad , \quad (19)$$

where  $C$  is a purely geometrical constant. Since the monotonic temperature dependence of  $i_c(T)$  does not significantly affect the response of the array near  $T_C$ , the behaviour of  $\delta V_{\omega}(T)$  in the transition region should reflect the characteristic features of  $\epsilon^{-1}(T, \omega)$  predicted by the dynamical extensions [33, 34] of the KT theory (see Sec. 2.2). This is quite clearly demonstrated by the peak in  $\text{Re}[\delta V_{\omega}(T)]$  and the drop in  $\text{Im}[\delta V_{\omega}(T)]$  shown in Fig.2 for the array A2. From these data, using an iterative procedure to solve Eq.(17), it is possible to extract  $\epsilon^{-1}(T, \omega)$ . The  $i_c(T)$  curves needed to calculate  $L_{K_{\alpha}}(T)$  were obtained by fitting low-temperature  $i_c$  measurements of A2 to the expression [43] :

$$i_c(T) = i_0 [1 - (T/T_{CS})]^2 \exp[-L/\xi_N(T)] \quad , \quad (20)$$

[using  $T_{CS} = 6.8$  K for the BCS transition temperature of the Pb islands,  $\xi_N(T_{CS}) = 1060$  Å for the Cu coherence length and  $i_0 = 0.38$  A] and by extrapolating the theoretical curves in the critical region. Results exhibiting the expected temperature dependence of  $\text{Re}(\epsilon^{-1})$  and  $\text{Im}(\epsilon^{-1})$  near the transition are shown in Fig. 3. A detailed comparison of these data with the theoretical predictions of Sec. 2.2 should shed further light on the dynamics of vortex excitations in 2D arrays.

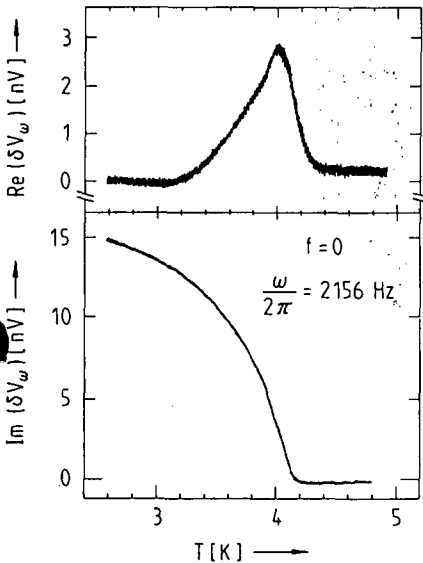


Fig.2 Temperature dependence of the complex ac response of array A2 in zero magnetic field ( $f = 0$ )

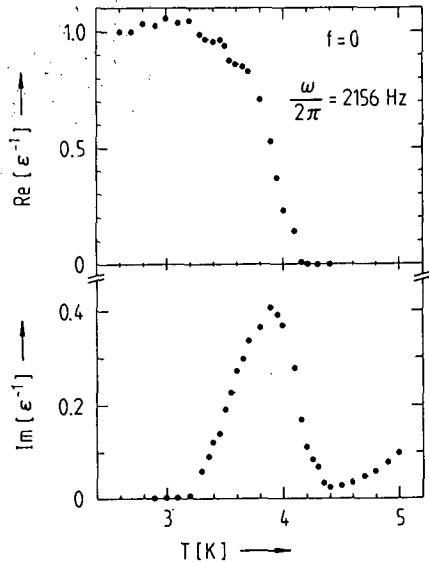


Fig.3 Temperature dependence of the inverse complex vortex dielectric constant of array A2 as deduced from the ac response shown in Fig.2 and from Eq. (17)

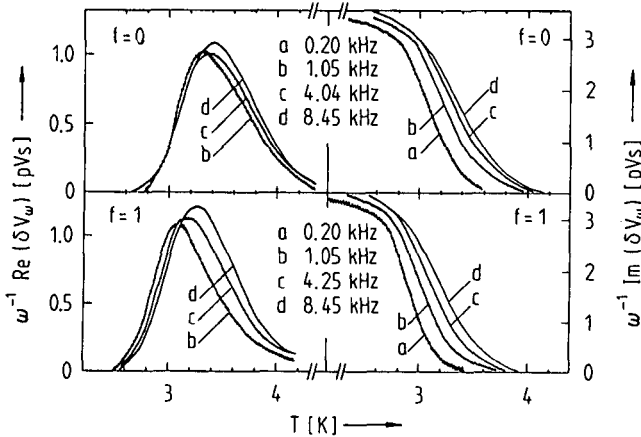


Fig.4 Temperature dependence of the normalized complex ac response of array A1 measured at different frequencies for  $f = 0$  and  $f = 1$ . From Ref. 13

As predicted by Eq.(12) and demonstrated by the  $f = 0$  ac response of A1 shown in Fig. 4, the peak in  $\text{Re}[\delta V_\omega(T)]$  shifts to higher temperatures and the fall-off of  $\text{Im}[\delta V_\omega(T)]$  broadens with increasing  $\omega$ . To analyze these results, we define  $\tilde{T}_\omega$  by extrapolating to zero the portions of the  $\text{Im}(\delta V_\omega)$  vs  $T$  curves [31] and introduce a scale parameter  $\lambda_\omega \equiv \ln(r_\omega/a)$ . Then, Eq. (12) can be written in the form :

$$\lambda_\omega^{-2} = b^{-2}(\tilde{T}_\omega - \tilde{T}_c) \quad (21)$$

The scale  $\lambda_\omega$  and the dimensionless temperature  $\tilde{T}_\omega = 2ek_B T_\omega / \hbar i_c(T_\omega)$  were calculated using, for A1,  $r_n = 2.2 \text{ m}\Omega$  to determine  $D_V$  and taking  $T_{CS} = 7 \text{ K}$ ,  $\xi_N(T_{CS}) = 850 \text{ \AA}$  and  $i_0 = 0.78 \text{ A}$  to deduce  $i_c(T_\omega)$  from Eq. (20). A plot for  $f=0$  of  $\lambda_\omega^{-2}$  vs  $\tilde{T}_\omega$  is shown in Fig. 5. A good fit to Eq. (21) is obtained for  $b = 1.29$ . Extrapolation of the linear plot to infinite scale ( $\omega \rightarrow 0$ ) leads to  $i_c(T_c)/T_c = 49 \text{ nA/K}$ . Inserting this result in the universal prediction (8) gives  $\epsilon_c = 1.75$ , a value in good agreement with an estimate ( $\epsilon_c = 1.81$ ) based on Monte Carlo simulations [38].

According to the KT picture discussed in Sec. 3, the response  $\delta V_\omega(T)$  for  $f = p \neq 0$  should be similar to that for  $f = 0$ , a conjecture confirmed by the experimental results for  $f = 1$  of A1 shown in Fig. 4. When compared with the case  $f = 0$ , however, the transition is seen to occur at a lower temperature. This is easily understood if one realizes that the finite size of the junction makes  $i_c$  field dependent. More precisely, the critical current of an isolated junction of the array is a quadratically decreasing function of the magnetic field as long as  $5B/\Phi_0 \ll 1$ , where  $S$  is an effective area of the junction. From Eq. (8), it then follows that the KT transition is pushed to lower temperatures by increasing  $f=p$ . The analysis of the frequency dependence of the response for  $f = 1$  shows, as demonstrated by the data of Fig. 5, that the vortex-unbinding transition at  $T_\omega$  shifts to higher temperatures with increasing  $\omega$  as predicted by Eq.(21). From the linear fit of Fig. 5, which was obtained using  $i_0(f=1) = 0.26 \text{ A}$  in Eq. (20), one deduces  $b(f=1) = 0.95$  and  $i_c(T_c, f=1)/T_c(f=1) = 143 \text{ nA/K}$ , a value leading to  $\epsilon_c(f=1) = 5.3$  [Eq.(8)]. Because of additional dielectric screening provided by the commensurate background of field-induced

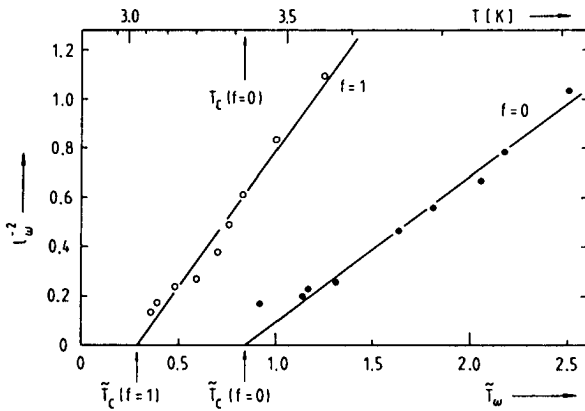


Fig. 5 Dependence of the scale parameter  $\lambda_\omega \equiv \ln(r_\omega/a)$  on the dimensionless vortex-unbinding temperature  $\tilde{T}_\omega$ . Solid lines are fits according to Eq.(21). The upper axis is a real temperature scale for  $f=0$ . From Ref.13

vortices, renormalization effects should be more important for  $f = 1$  than for  $f = 0$ , a conjecture consistent with the experimental observation  $\epsilon_c(f=1) > \epsilon_c(f=0)$ . Additional screening alone, however, seems to be insufficient to account for the large value of  $\epsilon_c$  found for  $f = 1$ .

The magnetic field dependence of the ac response  $\delta V_\omega$  has also been investigated [13]. In Fig. 6 we show the real and imaginary parts of  $\delta V_\omega$  measured at 4.033 kHz as a function of  $f$  for different temperatures. Prominent structures emerge in both  $\text{Re}[\delta V_\omega(f)]$  and  $\text{Im}[\delta V_\omega(f)]$  in correspondence to C-vortex phases defined by  $f = p$  and  $f = p/2$ . Structures at  $f = p/3$  are also clearly resolved in most of the data of Fig. 6. A detailed interpretation of these curves requires a theory describing the dynamics

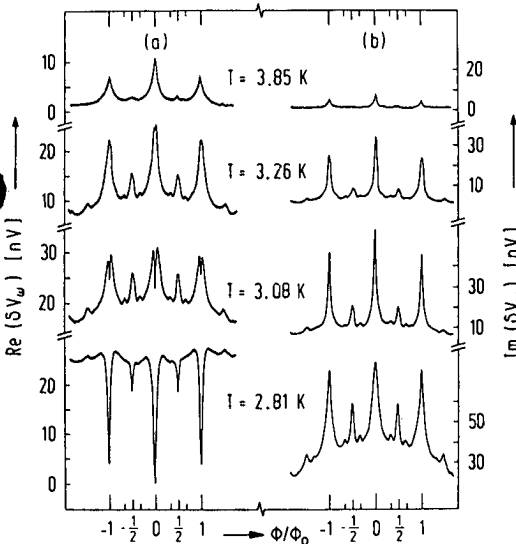


Fig. 6 (a) Real and (b) imaginary parts of the complex ac response at 4.033 kHz of array A1 as a function of the frustration parameter  $f = \Phi/\Phi_0$ . From Ref. 13

of field-induced vortices and of thermally generated topological excitations (vortices, domain walls, dislocations) in a periodic force field. Such a theory is not available so far. However, some of the essential features can be understood in terms of the "vortex picture" discussed in Sec. 3 and, for  $f = p$ , of the dynamics of thermally excited vortices. At low temperatures ( $T \ll T_C$ ), where the influence of topological excitations is negligible, structures in  $\delta V_\omega(f)$  at  $f = p/q$  reflect the drastic change in pinning occurring at a CI transition. As discussed in Sec. 3, in a low-order (small  $q$ ) C-phase the mobility of the field-induced vortices is considerably reduced by the periodic pinning potential provided by the array, while the vortex lattice can slide freely in an I-phase. As a consequence, there is a marked reduction of dissipation in a low-order C-phase, a process resulting in the periodic sequence of dips one observes in the  $\text{Re}[\delta V_\omega(f)]$  signals of Fig. 6 (a) at low temperatures. On the other hand, since pinning is important in low-order C-phases, considerable lag in response is expected for such vortex configurations. This is the mechanism responsible for the commensurate peaks occurring in the inductive component of  $\delta V_\omega(f)$  shown in Fig. 6 (b). As the temperature rises and approaches  $T_C(f)$ , the low-temperature commensurate dips in  $\text{Re}[\delta V_\omega(f)]$  gradually transform into peaks which finally vanish above  $T_C(f)$  [Fig. 6 (a)]. Simultaneously, a rapid degradation of the commensurate peaks in  $\text{Im}[\delta V_\omega(f)]$  is observed in the critical region [Fig. 6 (b)].

The evolution of the commensurate structures in  $\delta V_\omega(f)$  suggests the presence of thermally activated defects which, on account of their high mobility, generate additional dissipation and reduce the lag in response in a C-phase. We have shown that, for  $f=p$ , the dynamics of these defects has features allowing their identification as the vortex excitations of the KI theory. For a frustrated array ( $f=p/q$ ) further work is needed to ascertain the nature of the defects and their possible role in triggering the phase transition.

#### Acknowledgements

We thank G.-A. Racine for clarifying several aspects of the detection technique. This work was supported by the Swiss National Science Foundation.

#### References

1. J.M. Kosterlitz and D.J. Thouless : in Progress in Low-Temperature Physics, ed. by D.F. Brewer, Vol VII B (North-Holland, Amsterdam 1978) p. 371
2. R. Peierls : Helv. Phys. Acta 7 (Suppl. II), 81 (1934)
3. L.D. Landau : Zh. Eksp. Teor. Fiz. 7, 627 (1937)
4. N. Mermin and H. Wagner : Phys. Rev. Lett. 17, 1133 (1966)
5. P.C. Hohenberg : Phys. Rev. 158, 383 (1967)
6. J.M. Kosterlitz and D.J. Thouless : J. Phys. C 6, 1181 (1973)
7. D.J. Resnick, J.C. Garland, J.T. Boyd, S. Schoemaker, and R.S. Newrock : Phys. Rev. Lett. 47, 1542 (1981)
8. D.W. Abraham, C.J. Lobb, M. Thinkham, and T.M. Klapwijk : Phys. Rev. B 26, 5268 (1982)
9. M. Thinkham, D.W. Abraham, and C.J. Lobb : Phys. Rev. B 28, 6578 (1983)
10. D. Kimhi, F. Leyvraz, and D. Ariosa : Phys. Rev. B 29, 1487 (1984)
11. R.F. Voss and R.A. Webb : Phys. Rev. B 25, 3446 (1982)
12. R.A. Webb, R.F. Voss, G. Grinstein, and P.M. Horn : Phys. Rev. Lett. 51, 690 (1983)

13. Ch. Leemann, Ph. Lerch, G.A. Racine, and P. Martinoli : Phys. Rev. Lett. 56, 1291 (1986)
14. R.K. Brown and J.C. Garland : Phys. Rev. B 33, 7827 (1986)
15. B. Pannetier, J. Chaussy, and R. Rammal : J. Physique Lett. 44, L-853 (1983)
16. B. Pannetier, J. Chaussy, R. Rammal, and J.C. Villegier : Phys. Rev. Lett. 53, 1845 (1984)
17. S. Teitel and C. Jayaprakash : Phys. Rev. B 27, 598 (1983), and Phys. Rev. Lett. 51, 1999 (1983), and J. Physique Lett. 46, L-33 (1985)
18. W.Y. Shih and O. Stroud : Phys. Rev. B 28, 6575 (1983), and 30, 6774 (1984), and 32, 158 (1985)
19. M.Y. Choi and S. Doniach : Phys. Rev. B 31, 4516 (1985)
20. T.C. Hasley : Phys. Rev. B 31, 5728 (1985), and J. Phys. C 18, 2437, (1985), and Phys. Rev. Lett. 55, 1018 (1985)
21. D.H. Lee, J.D. Joannopoulos, J.W. Negele, and D.P. Landau : Phys. Rev. Lett. 52, 433 (1984), and Phys. Rev. B 33, 450 (1986)
22. V.S. Dotsenko and G.V. Uimin : J. Phys. C 18, 5019 (1985)
23. M. Yosefin and E. Domany : Phys. Rev. B 32, 1778 (1985)
24. E. Granato and J.M. Kosterlitz : Phys. Rev. B 33, 4767 (1986)
25. S. Miyashita and H. Shiba : J. Phys. Soc. Jpn. 53, 1145 (1984)
26. S. Alexander : Phys. Rev. B 27, 1541 (1983), and J. Physique 44, 805 (1983)
27. R. Rammal, T.C. Lubensky, and G. Toulouse : Phys. Rev. B 27, 2820 (1983)
28. R. Young : Phys. Rev. B 31, 4294 (1985)
29. O. Daldini, P. Martinoli, J.L. Olsen, and G. Berner : Phys. Rev. Lett. 32, 218 (1974)
30. A.T. Fiory, A.F. Hebard, and S. Somekh : Appl. Phys. Lett. 32, 73 (1978)
31. A.F. Hebard and A.T. Fiory : Phys. Rev. Lett. 44, 291 (1980), and Physica (Amsterdam) 109 & 110 B+C, 1637 (1982)
32. D.J. Bishop and J.D. Reppy : Phys. Rev. Lett. 40, 1727 (1978), and Phys. Rev. B 22, 5171 (1980)
33. V. Ambegaokar, B.I. Halperin, D.R. Nelson, and E. D. Siggia : Phys. Rev. Lett. 40, 783 (1978), and Phys. Rev. B 21, 1806 (1980)
34. S.R. Shenoy : J. Phys. C 18, 5163 (1985)
35. C.J. Lobb, D.W. Abraham, and M. Tinkham : Phys. Rev. B 27, 150 (1983)
36. J.E. Mooij : In Percolation, Localization, and Superconductivity, ed. by A.M. Goldman and S.A. Wolf, NATO ASI Series B, Phys. Vol. 109 (Plenum, New-York 1984) p. 325
37. J.M. Kosterlitz : J. Phys. C 7, 1046 (1974)
38. J. Tobochnik and G.V. Chester : Phys. Rev. B 20, 3761 (1979)
39. J.C. Lobb : Physica (Amsterdam) 126B, 319 (1984)
40. J. Villain : J. Phys. C 10, 1717 and 4793 (1977)
41. A.T. Fiory and A.F. Hebard : in Inhomogeneous Superconductors, ed. by O.U. Gubser, T.L. Francevillia, S.A. Wolf, and J.R. Leibowitz, AIP Conference Proceedings No 58 (American Institute of Physics, New York 1980) p. 293
42. Ch. Leemann, Ph. Lerch, G.A. Racine, A. Strupler, and P. Martinoli : in SQUID 85, ed. by H.D. Hahlbohm and H. Lübbig (Walter de Gruyter, Berlin 1985) p. 1065
43. P.G. de Gennes : Rev. Mod. Phys. 36, 225 (1964)

THE KOSTERLITZ-THOULESS TRANSITION

IN JOSEPHSON JUNCTION ARRAYS

Ch. Leemann, Ph. Lerch, R. Theron and P. Martinoli

Institut de Physique, Université de Neuchâtel, 2000 Neuchâtel, Switzerland

Abstract : A study of the ac response of square two-dimensional arrays of proximity effect Josephson junctions as a function of temperature, frequency and applied transverse magnetic field is presented. As a function of magnetic field, both the real and the imaginary part of the array's conductance exhibit clear structures at fields corresponding to rational numbers of flux quanta per unit cell of the array. At an integer number of flux quanta per unit cell, the temperature and frequency dependence of the conductance show that the superconducting to normal transition of the array can be described by the Kosterlitz-Thouless theory and by its extension to finite frequencies.

I. Introduction

The Kosterlitz-Thouless (KT) theory of phase transitions [1,2], applied to a two-dimensional (2D) superconductor [3], is based on a description of the superconductor in terms of fluctuations in the phase of its order parameter. At low temperatures the relevant phase fluctuations are slowly varying functions of position. As the temperature increases, thermal fluctuations in the phase result in topological excitations in the form of bound pairs of vortices of opposite circulation (vortex-antivortex pairs). The transition to the normal state is triggered by the unbinding of these vortex pairs, i.e. the creation of free vortices at a critical temperature  $T_c$ . The most obvious consequence of such a transition is the appearance of a dc resistance with a characteristic temperature dependence [4-8] above  $T_c$ . Another mani-

festation of the KT transition is the crossover in behavior one observes in the sample's current-voltage characteristics in the vicinity of  $T_C$  [7,9]. In the transition region the dynamics of vortex excitations has unique features which can be seen in experiments probing the response of 2D systems exposed to ac driving fields [10,11]. In particular, measurements of the complex dynamic sheet conductance allow to verify two important theoretical predictions : the temperature dependence of the complex dielectric constant, and the anomalous temperature dependence of the free vortex correlation length above  $T_C$ . In this paper we report measurements of the complex conductance of proximity-coupled 2D arrays of Josephson junctions [12]. In section II we introduce the basic concepts of the KT transition. Section III is dedicated to array physics. We discuss the relationship between arrays and the XY model, some vortex dynamics and magnetic field effects. Our experimental procedures and results are presented in section IV. The results are analyzed within the theoretical framework of sections II and III. Section V contains our conclusions.

## II. Basic features of the KT transition

Consider the classical XY model : a regular lattice of spins on the XY-plane. The spins are subject to nearest neighbor interactions and are free to rotate about an axis perpendicular to the XY-plane. The  $i$ th spin is described by  $\phi_i$ , the angle it makes with a fixed direction in the XY-plane. The Hamiltonian of the system is given by

$$H = -J \sum_{\langle i,j \rangle} \cos(\phi_j - \phi_i) \quad , \quad (1)$$

where the sum is over all pairs of spins and  $J$  (positive) is the coupling energy. Except at zero temperature, where all the spins are aligned, there is no conventional long-range order in the spin system and thus a vanishing spontaneous magnetization [13]. In fact, at any non-zero temperature spin waves (i.e. long wavelength excitations of the spins) lead, at large enough distances, to uncorrelated spins. On the other hand, at sufficiently low temperatures, we are not in the presence of liquid-like short range order. Wegner

[14] found that the spin-spin correlation function decays algebraically, with a temperature dependent exponent  $\eta(T) = k_B T / 2\pi J$  :

$$\langle \cos(\phi_j - \phi_i) \rangle \propto r_{ij}^{-\eta(T)}, \quad (2)$$

where  $r_{ij}$  is the distance between the lattice sites  $i$  and  $j$ . Intuitively, one expects some type of phase transition from a low temperature phase characterized by the quasi long-range order described by (2) to a high temperature liquid-like phase characterized by an exponentially decaying correlation function. This phase transition was investigated by Kosterlitz and Thouless in 1972 [1] by taking into account the effects of thermally excited vortices. A vortex (antivortex) is defined as a configuration of the  $\phi_i$  such that the sum of the phase changes along a closed path is  $2\pi$  ( $-2\pi$ ). The energy  $E_V$  of an isolated vortex can be computed from (1) and is given by

$$E_V = \pi J \log L/a, \quad (3)$$

where  $L$  is the system size and  $a$  the lattice parameter. For the interaction energy  $E_p$  of a vortex-antivortex pair with cores separated by a distance  $r$ , one finds

$$E_p = 2\pi J \log r/a. \quad (4)$$

Notice that in general  $E_p \ll E_V$ , the thermal excitation probability is therefore larger for bound pairs than for single vortices. A rough estimate [1] of the KT transition temperature  $T_c$  can be obtained by computing the free energy  $F = E_V - TS$  of a single vortex excitation and by requiring that at  $T = T_c$  there is a spontaneous nucleation of free vortices, i.e.  $F(T_c) = 0$ . This leads to  $k_B T_c \approx \pi J / 2$ . The correct value for  $T_c$  is obtained by taking into account the presence of bound pairs and their interaction. The interaction between the constituents of a pair of size  $r_0$  is reduced ("renormalized") by an amount  $\epsilon(r_0)$ , due to the presence of pairs of size  $r < r_0$ . The calculation of renormalized quantities, which is the main scope of the theory, is based on the KT scaling equations [1]. The physical interpretation of  $\epsilon(r)$  becomes obvious by making an analogy with the 2D Coulomb

gas, where electric charges also interact logarithmically [1,6,15]. In the 2D Coulomb gas analogue,  $\epsilon(r)$  describes the scale dependent screening properties of a dielectric medium consisting of electric dipoles (corresponding to the vortex-antivortex pairs in the XY model) of different size.

Thus we have the following picture for the KT-transition : at low temperatures there are thermal excitations in the form of spin waves and bound vortex-antivortex pairs. At a transition temperature  $T_C$  given by

$$2k_B T_C = \pi J_R \quad , \quad (5)$$

where  $J_R = J/\epsilon_C$  is the renormalized coupling energy and  $\epsilon_C$  the dielectric constant at infinite scale  $\epsilon(\infty)$ , pairs of largest separation ( $r \rightarrow \infty$ ) unbind. The resulting free vortex excitations (corresponding to free electric charges in the 2D Coulomb gas analogue) destroy the quasi long-range order existing below  $T_C$ . Above  $T_C$  one is dealing with a liquid-like phase characterized by a correlation function of the form

$$\langle \cos(\phi_j - \phi_i) \rangle \propto e^{-r_{ij}/\xi_+(T)} \quad . \quad (6)$$

The correlation length  $\xi_+(T)$  has an unusual temperature dependence reflecting the peculiar nature of the KT transition. It is given by [2]

$$\xi_+(T) \approx a e^{b[T - T_C]^{-1/2}} \quad , \quad (7)$$

where  $b$  is a nonuniversal constant of order unity. Physically,  $\xi_+(T)$  is a measure of the average separation of free vortices. The free vortex areal density  $n_f$  is therefore approximately given by  $n_f \approx \xi_+^{-2}(T)$ .

### III. 2D Arrays

#### a) Connection with the XY model

Large two-dimensional arrays of superconducting weak links constitute a very appealing physical realization of the XY model. With modern photolitho-

graphic techniques it is possible to fabricate large regular lattices of superconducting (S) islands. The individual islands are Josephson coupled through an insulator (I) forming arrays of SIS junctions [16] or through a normal metal (N), forming proximity effect SNS arrays [17-19]. In arrays where the geometrical and physical properties of the individual junctions are sufficiently uniform, fluctuations in the magnitude of the superconducting order parameter are largely suppressed well below the BCS transition of the individual islands. On the other hand, 2D fluctuations in the phase of the order parameter are still important. The phase difference ( $\phi_j - \phi_i$ ) between two sites and its time evolution are governed by the Josephson equations. The supercurrent flowing between islands  $i$  and  $j$  is given by

$$i_s = i_c(T) \sin(\phi_j - \phi_i) \quad ,$$

where  $i_c(T)$  is the critical current of the junction. The voltage across the barrier is

$$V = \frac{\hbar}{2e} \frac{\partial}{\partial t} (\phi_j - \phi_i) \quad .$$

With these two expressions the interaction energy  $E_{ij} = \int i_s V dt$  of the islands  $i$  and  $j$  becomes :

$$E_{ij} = \frac{\hbar i_c(T)}{2e} [1 - \cos(\phi_j - \phi_i)] \quad . \quad (8)$$

Summing over all pairs  $\langle ij \rangle$  we obtain the same Hamiltonian as in (1), with a coupling energy

$$J = \frac{\hbar i_c(T)}{2e} \quad . \quad (9)$$

The phase of the superconducting order parameter corresponds to the spin-angle variable of the XY model. With (5), the universal KT prediction for the transition temperature becomes

$$\frac{i_c(T_c)}{e_c T_c} = \frac{8ek_B}{h} \approx 27 \text{ nA/K} \quad . \quad (10)$$

Since the coupling energy in (9) is temperature dependent, the statistical

mechanics of the system is conveniently described in terms of a dimensionless temperature parameter  $\tilde{T} = k_B T / J = 2ek_B T / (\hbar i_c(T))$  [20]. In particular it is  $\tilde{T}$  and not  $T$ , which enters expression (7) for  $\xi_+$ .

There is one important limitation to the isomorphism between the XY model and 2D arrays. In 2D arrays, as in all 2D superconductors, the vortex-antivortex interaction no longer depends logarithmically on the separation distance at distances larger than the effective penetration depth  $\Lambda$  [21]. It turns out, however, that at  $T_C$ ,  $\Delta T_C \approx 2 \text{cmK}$  [20]; in the interesting temperature region  $\Lambda$  is therefore a macroscopic length scale.

#### b) Vortex dynamics in arrays

The dynamical properties of the KT transition were studied by Ambegaokar et al [22,23]. An important result of their model is that the vortex response to an applied field of angular frequency  $\omega$  is controlled by a frequency dependent length  $r_\omega = (14D/\omega)^{1/2}$ , where  $D$  is the vortex diffusion constant. Bound vortex pairs of size larger than  $r_\omega$  do not respond to the applied field, whereas the response of the smaller pairs ( $r < r_\omega$ ) is described by a complex dielectric constant which is derived from the static KT dielectric constant  $\epsilon(r)$  in the following way [22,23] :

$$\begin{aligned} \text{Re } \epsilon(\omega) &= \epsilon(r_\omega) \\ \text{Im } \epsilon(\omega) &= \frac{\pi}{4} \left( r \frac{d\epsilon}{dr} \right) \Big|_{r=r_\omega} \end{aligned} \quad (11)$$

According to the physical interpretation of  $\xi_+(\tilde{T})$ , at finite frequencies the vortex unbinding transition will be seen at a temperature  $T_\omega$  such that

$$r_\omega = \xi_+(\tilde{T}_\omega) \quad (12)$$

By making use of the 2D Coulomb gas analogue, the contribution,  $\epsilon_f$ , of the free vortex charges to the dielectric constant above  $T_C$  can be written in the form

$$\epsilon_f = i \frac{4\pi \sigma_V}{\omega} \quad , \quad (13)$$

where  $\sigma_v = (e/h)r_{\Omega}i_c(T)[a^2/\xi_+^2(T)]$  is the free vortex conductivity [12], proportional to  $n_f \approx \xi_+^{-2}(T)$ , and  $r_{\Omega}$  is the resistance of an individual junction.

In the experiments reported below (section IV), the physical quantity of interest is the complex sheet impedance,  $Z_{\Omega}(\omega, T)$  of the array. It is related to the complex vortex dielectric constant  $\epsilon(\omega, T)$  by

$$Z_{\Omega}(\omega, T) = i\omega L_{K\Omega}\epsilon(\omega, T) \quad (14)$$

where  $L_{K\Omega} = \hbar/(2ei_c(T))$  is the sheet kinetic inductance of the array and  $\epsilon(\omega, T) = \epsilon'(\omega, T) + i\epsilon''(\omega, T)$  with, according to Eqs. (11) and (12),  $\epsilon'(\omega, T) = \epsilon(r_{\omega})$  and  $\epsilon''(\omega, T) = \pi/4[r_{\omega}(d\epsilon/dr)|_{r=r_{\omega}}] + 4\pi\sigma_v/\omega$ .

c) Magnetic field effects

A magnetic field  $\vec{B}$ , perpendicular to the plane of the array, introduces vortices with a tendency to form a regular 2D lattice, the lattice parameter being controlled by the magnitude of  $\vec{B}$ . The interaction of the field-induced vortices with the periodic pinning potential provided by the array leads to commensurate (C) and incommensurate (I) vortex phases. The array can now be described by a uniformly frustrated lattice spin model [24-27], with a Hamiltonian

$$H = -J \sum_{\langle ij \rangle} \cos(\phi_j - \phi_i - A_{ij}) \quad (15)$$

where the argument of the cosine is the gauge-invariant phase difference between islands  $i$  and  $j$ ,  $\phi_0 A_{ij}/(2\pi)$  is the line integral of the vector potential  $\vec{A}$  from site  $i$  to site  $j$  and  $\phi_0$  is the superconducting flux quantum. The  $A_{ij}$ 's satisfy the condition  $\oint A_{ij} = 2\pi f$ , where the sum is over all the links in an elementary cell and  $f$ , the frustration parameter, represents the magnetic flux per elementary cell in units of  $\phi_0$ :  $f = Ba^2/\phi_0$ . If the magnetic field is uniform,  $f$  is a constant over the entire array. Quite clearly, the Hamiltonian (15) is periodic in  $f$  with period 1. Furthermore, as  $f$  changes, the energy of the system goes through a series of local minima, corresponding to rational values of  $f$  (C-vortex phases). As a consequence, the transition temperature and the critical currents show a complex periodic dependence on  $f$  [24, 27-29].

#### IV. Experimental results and discussion

Arrays consisting of  $N \times N$  Pb/Cu proximity-effect junctions, with  $N \approx 10^3$ , were fabricated on sapphire substrates using standard evaporation techniques, photolithography and sputter-etching. Fig. 1 shows a scanning electron micrograph of a typical array. The square lead islands, 200 nm thick, form a square lattice on a 200 nm thick copper film. The lattice parameter  $a$  is  $8 \mu\text{m}$ , the distance  $L$  between the squares is  $1.7 \mu\text{m}$ . Fig. 2 shows the resistance of an array as a function of temperature. There are two distinct transitions, as observed by other groups [17-19]: the proximity-effect reduced BCS transition of the lead islands at 6.8 K and a transition to zero resistance at  $T_c \approx 3.9$  K. In the temperature region  $3.9 \text{ K} < T < 6.8 \text{ K}$  the coherence length in the copper increases with decreasing temperature leading to an increase of the effective size of the superconducting islands and thereby a decrease in resistance [17].

The complex sheet conductance  $G_{\square} = Z_{\square}^{-1}$  of the arrays was measured using a variation of the mutual inductance technique devised by Fiory and Hebard [11,30]. Two coaxial cylindrical coils consisting of an external drive coil of diameter 4 mm and an internal astatic pair of receive coils, 2 mm in diameter, were immersed in stycast. After appropriate machining, the coil assembly was positioned directly on the sample, the distance between the sample and the first winding of the detection coil being of the order of  $10 \mu\text{m}$ . An

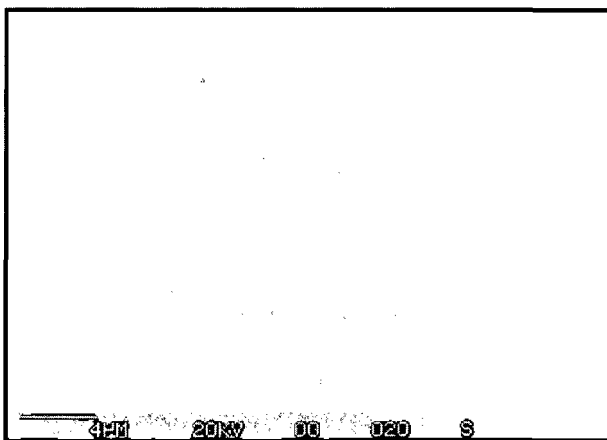


Figure 1. Scanning electron micrograph of an array. Lighter colored squares are the Pb islands on the top of the darker Cu film.

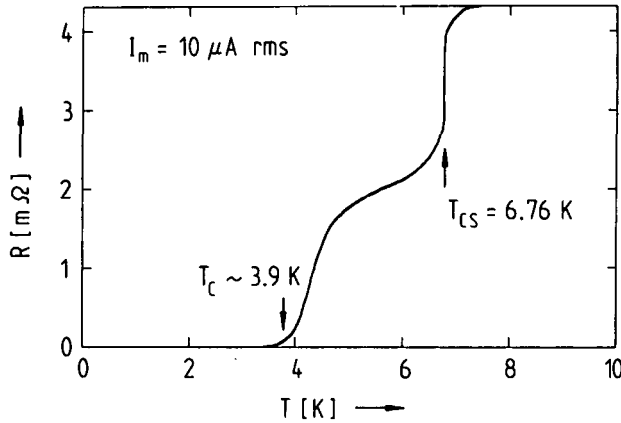


Figure 2. Dc resistance vs temperature of a 2D array of Josephson junctions.  $T_{CS}$  : BCS-transitions of the Pb islands.  $T_C$  : Vortex unbinding transition.

ac current of amplitude  $I_{D\omega}$  and angular frequency  $\omega$  flowing through the drive coil will induce screening currents in the array proportional to  $I_{D\omega}$  and  $\omega$  and, in the weak screening limit [30], also to  $G_{\square}$ , the complex sheet conductance of the array. These currents will, in turn, induce a voltage  $\delta V_{\omega} \propto \omega^2 I_{D\omega} G_{\square}$  at the receive coil which can be phase-sensitively detected. Using Eq. (14) for  $G_{\square} = Z_{\square}^{-1}$ , in the weak screening limit appropriate to discuss our experiments in the transition region, the signal voltage can be written as :

$$\delta V_{\omega}(T) = iC\omega I_{D\omega} \frac{i_C(T)}{\epsilon(\omega, T)}, \quad (16)$$

where  $C$  is a constant depending on the sample-coil geometrical configuration, whose numerical value was estimated to be  $\sim 0.74 \text{ Vs/A}^2$ . At low temperatures ( $T \ll T_C$ ) the weak screening condition is no longer satisfied and Eq.(16) must be modified to include the geometrical inductance of the sample.

Since  $i_C(T)$  is a monotonically decreasing function of temperature, any unusual behaviour of the signal voltage  $\delta V_{\omega}$  in the transition region will be determined by  $\epsilon^{-1}(\omega, T)$ . Calculations of  $\epsilon^{-1}(\omega, T)$  based on Eqs. (11)

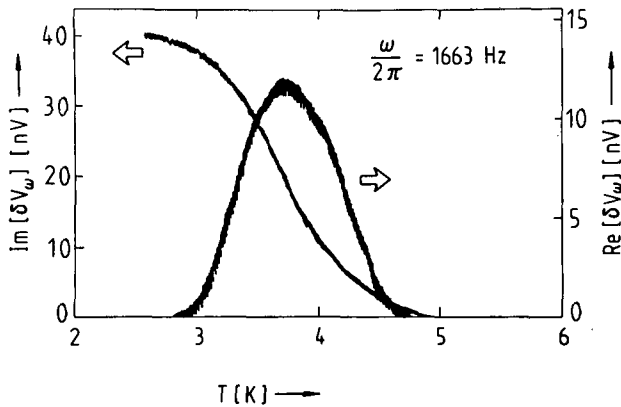


Figure 3. Temperature dependence of the receive coil signal  $\delta V_\omega$  proportional to the array's sheet conductance at a frequency of 1663 Hz.

and (13) show that a peak in  $\text{Im}(\epsilon^{-1})$  and a roll-off in  $\text{Re}(\epsilon^{-1})$  are expected in the neighborhood of  $T_c$ . This is quite clearly demonstrated by the measurements shown in Fig. 3 which exhibit a peak in dissipation [ $\text{Re}(\delta V_\omega)$ ] and a drop in superfluid density [ $\text{Im}(\delta V_\omega)$ ]. Structures similar to those shown in Fig. 3 were observed in uniform 2D superconductors [11] and in superfluid helium films [10].

The evolution of the signals with increasing frequency is shown in Fig. 4, where the signal voltage is normalized with respect to the angular frequency of the driving current. Notice that, with increasing frequency, the structures in both  $\text{Re}(\delta V_\omega)$  and  $\text{Im}(\delta V_\omega)$  shift to higher temperatures. This is consistent with the theoretical prediction implied by Eq. (12): as the frequency increases, the probing length  $r_\omega$  becomes smaller and the vortex unbinding transition is observed at a higher temperature  $T_\omega$ .

Also shown in Fig. 4 are the signals measured in a magnetic field corresponding to one flux quantum per unit cell of the array, the  $f = 1$  case. The response for  $f = 1$  is similar to that for  $f = 0$ , in qualitative agreement with the conclusion of section III, that the Hamiltonian of the system is periodic in  $f$  with period 1. We conjecture that in the  $f = 1$  case the thermal excitations are highly mobile positive and negative vacancies, which can be viewed as vortex-antivortex excitations superposed on a pinned commensurate background of one field-induced vortex per unit cell of the array. Notice however, that the transition for  $f = 1$  in Fig. 4 occurs at a slightly lower

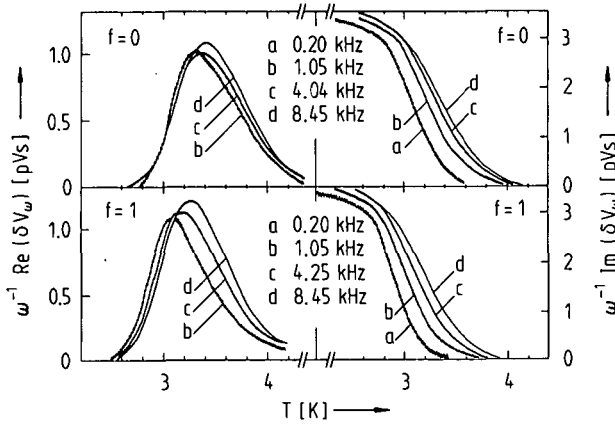


Figure 4. Temperature dependence of the complex ac response of a 2D array at different frequencies for  $f=0$  and  $f=1$ . Signal voltages are normalized with respect to angular frequency.

temperature than in the  $f = 0$  case. The finite size of the junctions causes the critical current of the individual junctions to be slightly reduced by the magnetic field. The KT transition is thus also expected to occur at a slightly reduced temperature in the case  $f = 1$ .

The frequency dependence of the signals, through Eq. (12), can be used to verify the unusual temperature dependence of the vortex correlation length  $\xi_+(T)$  given in Eq. (7). The  $r_\omega$ -values were calculated with  $D = (c/\phi_0)^2 r_n a^2 k_B T$  for the vortex diffusivity, as derived in Ref. 20, and  $r_n = 2.2 \text{ m}\Omega$ , inferred from the array sheet resistance at  $T_{CS}^-$ . The temperatures  $T_\omega$  were deduced from the  $\text{Im}(\delta V_\omega)$  vs  $T$  curves by extrapolating the steep portions to zero. In order to determine  $\tilde{T} = k_B T/J = 2ek_B T/(\hbar i_C(T))$ , low temperature measurements of the array's critical current in zero field,  $i_C(T,0)$ , and in a  $f = 1$  field,  $i_C(T,1)$ , were fitted to the expression

$$i_C(T,f) = i_0(f) [1 - (T/T_{CS})]^2 \exp[-L/\xi_N(T)], \quad (17)$$

yielding  $\xi_N(T_{CS}) = 85 \text{ nm}$  for the Cu coherence length,  $i_0(0) = 0.78 \text{ A}$  and  $i_0(1) = 0.26 \text{ A}$ . Finally, introducing the scale parameter  $\ell_\omega = \ln(r_\omega/a)$ ,

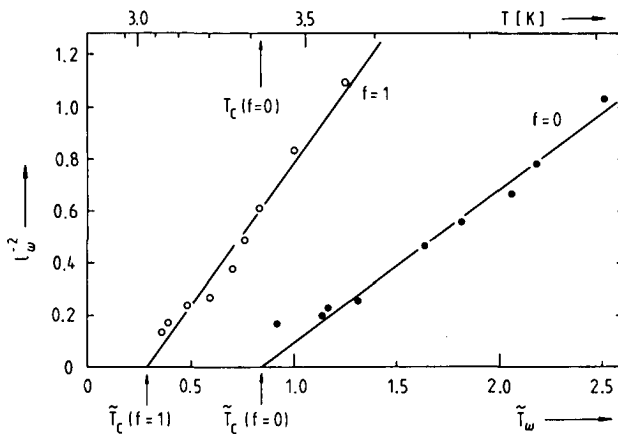


Figure 5. Dependence of the scale parameter  $\lambda_\omega = \lambda n(r_\omega/a)$  on the dimensionless temperature  $\tilde{T}_\omega$ . Solid lines are fits according to Eq. (18). On the upper axis the real temperature for  $f = 0$  is shown.

Eq. (12) can be cast into the form

$$\lambda_\omega^{-2} = b^{-2}[\tilde{T}_\omega - \tilde{T}_c(f)] \quad , \quad (18)$$

As can be seen in Fig. 5, our measurements confirm the linear relationship between  $\lambda_\omega^{-2}$  and  $\tilde{T}_\omega$ . By extrapolating the fitted straight lines to infinite scale, corresponding to the limit  $\omega \rightarrow 0$ , we find  $i_c(T_c, 0)/T_c(0) = 49 \text{ nA/K}$  and  $i_c(T_c, 1)/T_c(1) = 143 \text{ nA/K}$ , which leads, with Eq. (10), to  $\epsilon_c(0) = 1.81$  and  $\epsilon_c(1) = 5.3$ . Our  $\epsilon_c(0)$  value is in excellent agreement with a Monte Carlo calculation performed by Tobochnik and Chester [31], who found  $\epsilon_c = 1.75$ . The  $\epsilon_c(1)$  value, on the other hand, seems somewhat large, even though additional screening by the commensurate vortex background is expected to enhance  $\epsilon_c$ .

At this point, having studied the temperature dependence of the response at integer values of  $f$ , we would like to consider the dynamic response of the array also at rational and irrational values of  $f$ . Real and imaginary parts of the signal as a function of the frustration parameter  $f$  are shown in Fig. 6 at four different temperatures. The structures occurring at integer  $f$

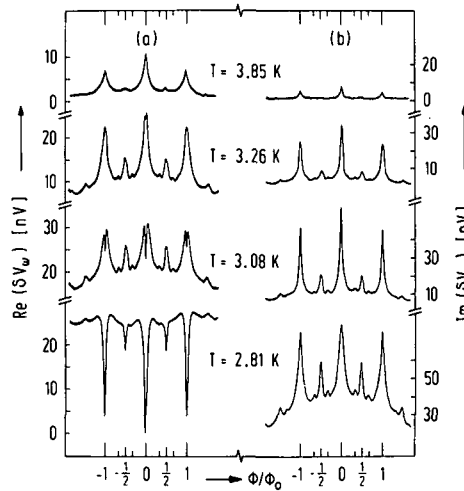


Figure 6. (a) Real and (b) imaginary parts of the ac response at 4033 Hz as a function of the frustration parameter  $f = \phi/\phi_0$  at four temperatures

values, as well as half-integer  $f$  values ( $f=p/2$ ) and at  $f=p/3$ , reveal the presence of low energy commensurate vortex phases. At integer  $f$  values the evolution of the structures with temperature is the signature of the vortex-unbinding transition discussed above. The temperature evolution of the signals at low-order rational  $f$  values is similar to that observed at integer  $f$  values, leading to speculations about the possibility of a KT-like phase transition at rational values of  $f$ . However, a theory describing the dynamics of field-induced vortices and their interaction with topological excitations such as thermal vortices and domain walls at non-zero temperatures is not available. A detailed analysis of the data shown in Fig. 6 is therefore not yet possible.

## V. Conclusions

Our measurements of the dynamic response of 2D arrays, in magnetic fields corresponding to integer values of the frustration parameter  $f$ , as a function of temperature verify the qualitative behavior of the dielectric constant  $\epsilon(\omega, T)$  predicted by the KT theory for phase transitions in two

dimensions. The analysis of the frequency dependence of the measurements provides a quantitative check of the exponential-inverse-square-root temperature dependence of the free vortex correlation length above  $T_c$ .

The nature of the phase transition in magnetic fields corresponding to non-integer  $f$  values is an unsolved and challenging problem. In particular, the case  $f = 1/2$ , corresponding to the fully frustrated XY model, has recently received a considerable amount of attention and some progress is being made, both theoretically and with numerical computer simulations [27, 32, 33]. Our experimental work to-date on 2D arrays cannot unambiguously settle the question of the nature of the phase transition, KT-like or Ising-like at  $f = 1/2$ .

This work was supported by the Swiss National Science Foundation.

#### References

- [1] J.M. Kosterlitz and D.J. Thouless, J. Phys. C 6, 1181 (1973); and in Progress in Low Temperature Physics, vol. VII B, ed. by D.F. Brewer (North Holland, 1978), p. 371
- [2] J.M. Kosterlitz, J. Phys. C 7, 1046 (1974)
- [3] M.R. Beasley, J.E. Mooij and T.P. Orlando, Phys. Rev. Lett. 42, 1165 (1979)
- [4] L.A. Turkevich, J. Phys. C 12, L385 (1979)
- [5] B.I. Halperin and David R. Nelson, J. Low Temp. Phys. 36, 599 (1979)
- [6] S. Doniach and B.A. Huberman, Phys. Rev. Lett. 42, 1169 (1979)
- [7] K. Epstein, A.M. Goldman and A.M. Kadin, Phys. Rev. Lett. 47, 534 (1981) and Phys. Rev. B 26, 3950 (1982)
- [8] S.A. Wolf, D.V. Gubser, W.W. Fuller, J.C. Garland and R.S. Newrock, Phys. Rev. Lett. 47, 1071 (1981)
- [9] A.F. Hebard and A.T. Fiory, Phys. Rev. Lett. 50, 1603 (1983)
- [10] D.J. Bishop and J.D. Reppy, Phys. Rev. Lett. 40, 1727 (1978) and Phys. Rev. B 22, 5171 (1980)
- [11] A.F. Hebard and A.T. Fiory, Phys. Rev. Lett. 44, 291 (1980); and Physica (Amsterdam) 109&110 B+C, 1637 (1982)

- [12] Ch. Leemann, Ph. Lerch, G.-A. Racine and P. Martinoli, Phys. Rev. Lett. 56, 1291 (1986)
- [13] N.W. Ashcroft and N.D. Mermin, Solid State Physics (Saunders, Philadelphia, 1976)
- [14] F. Wegner, Z. Phys. 206, 465 (1967)
- [15] P. Minnhagen, Phys. Rev B 23, 5745 (1981)
- [16] R.F. Voss and R.A. Webb, Phys. Rev. B 25, 3446 (1982)
- [17] D.J. Resnick, J.C. Garland, J.T. Boyd, S. Shoemaker and R.S. Newrock, Phys. Rev. Lett. 47, 1542 (1981)
- [18] D.W. Abraham, C.J. Lobb, M. Tinkham and T.M. Klapwijk, Phys. Rev. B 26, 5268 (1982)
- [19] D. Kimhi, F. Leyvraz and D. Ariosa, Phys. Rev. B 29, 1487 (1984)
- [20] C.J. Lobb; D.W. Abraham and M. Tinkham, Phys. Rev. B 27, 150 (1983)
- [21] P.G. De Gennes, Superconductivity of metals and alloys, (Benjamin, New-York, 1966)
- [22] V. Ambegaokar, B.I. Halperin, D.R. Nelson and E.D. Siggia, Phys. Rev. Lett. 40, 783 (1978) and Phys. Rev. B 21, 1806 (1970)
- [23] V. Ambegaokar and S. Teitel, Phys. Rev. B 19, 1667 (1979)
- [24] S. Teitel and C. Jayaprakash, Phys. Rev. B 27, 598 (1983) and Phys. Rev. Lett. 51, 1999 (1983)
- [25] W.Y. Shih and D. Stroud, Phys. Rev. B 28, 6575 (1983) and 30, 6774 (1984) and 32, 158 (1985)
- [26] M.Y. Choi and S. Doniach, Phys. Rev. B 31, 4516 (1985)
- [27] T.C. Halsey, Phys. Rev. B 31, 5728 (1985) and Phys. Rev. Lett. 55, 1018 (1985) and J. Phys. C 18, 2437 (1985)
- [28] M. Tinkham, D.W. Abraham and C.J. Lobb, Phys. Rev. B 28, 6578 (1983)
- [29] B. Pannetier, J. Chaussy, R. Rammal and J.C. Villegier, Phys. Rev. Lett. 53, 1845 (1984)
- [30] A.T. Fiory and A.F. Hebard, in Inhomogeneous Superconductors - 1979, ed. by D.U. Gubser, T.L. Francavilla, S.A. Wolf and J.R. Leibovitz, AIP Conference Proceedings No 58 (American Institute of Physics, New-York, 1980), p. 293
- [31] J. Tobochnik and G.V. Chester, Phys. Rev. B 20, 3761 (1979)
- [32] D.H. Lee, J.D. Joannopoulos, J.W. Negele and D.P. Landau, Phys. Rev. B 33, 450 (1986)
- [33] M. Yosefin and E. Domany, Phys. Rev. B 32, 1778 (1985)

DYNAMIC CONDUCTANCE OF TWO-DIMENSIONAL  
ARRAYS OF JOSEPHSON JUNCTIONS

Ph. Lerch, R. Théron, Ch. Leemann and P. Martinoli  
Institut de Physique, Université de Neuchâtel,  
2000 Neuchâtel, Switzerland

Abstract

The ac sheet conductance of large two-dimensional arrays of proximity effect SNS Josephson junctions was measured as a function of temperature, frequency and applied perpendicular magnetic field. A quantitative analysis of the data shows that the normal to superconducting transition of unfrustrated arrays follows the predictions of the Kosterlitz-Thouless theory for phase transitions in two dimensions.

1. Introduction

A two-dimensional (2D) array of weakly coupled Josephson junctions in zero magnetic field provides a physical realization of the XY-model<sup>1</sup>. For this system, the Kosterlitz-Thouless (KT) theory predicts a transition from a low temperature phase, exhibiting quasi long-range order, to a high temperature, disordered phase<sup>2</sup>. The phase transition is triggered by the unbinding of vortex-antivortex pairs, a process creating free vortices at a critical temperature  $T_c$ . Experimental studies of the resistive transition and of current-voltage characteristics of 2D arrays were found to be consistent with a KT-like transition<sup>3-6</sup>.

In a weak perpendicular magnetic field, a 2D array of weak links becomes equivalent to a uniformly frustrated XY-model<sup>7-11</sup>, with a frustration parameter given by the ratio of the magnetic flux  $\phi$  threading an elementary cell of the array and the superconducting flux quantum  $\phi_0 = hc/2e$ :  $f = \phi/\phi_0$ . The ground state energy of the array was found to be periodic in  $f$  with period 1, exhibiting local minima at rational  $f$ <sup>7-10</sup>, a property verified by measurements of critical currents and transition temperatures as a function of  $f$ <sup>5,6,12</sup>.

The nature of the phase transition at non integer  $f$  values is presently subject of intense theoretical investigation. At rational  $f$ -values there are, in addition to point defects (i.e. vortices), topological excitations in the form of line defects (domain walls). It is not clear whether the phase transition will be dominated by the unbinding of point defects (KT-like transition) or by the proliferation of domain walls (Ising-like transition) or, indeed, by some combination of the two<sup>7-11,13-15</sup>.

The dynamics of vortex excitations in a 2D system undergoing a phase transition has unique features which can be tested with an experiment probing the ac response of the vortex medium. With a two-coil mutual inductance technique<sup>16</sup>, we have studied<sup>17</sup> the dynamics of the phase transition in 2D arrays of proximity effect Pb/Cu/Pb junctions. Comparison of our experimental results with the predictions of the KT-theory<sup>2</sup> and its extension to finite frequencies<sup>18</sup>, provided detailed and quantitative support in favour of a KT-like transition in magnetic fields corresponding to integer values of  $f$ . In the present paper, in addition to describing some experimental aspects of our work, we report some further quantitative analyses of our data.

Manuscript received September 30, 1986

2. Sample Preparation

A small section of an array of  $N \times N$ ,  $N \approx 10^3$ , Pb/Cu/Pb proximity-effect Josephson junctions is shown in Fig. 1. The Pb islands form a square lattice with lattice parameter  $a = 8\mu\text{m}$  on the Cu film, the distance between adjacent Pb squares is  $L = 1.7\mu\text{m}$ . The Cu and Pb films, each about 2000 Å in thickness, were evaporated using two independent power supplies, so that no more than 1 second of time elapsed between the two evaporations. This ensured a good proximity effect between the two metals. The square array was then patterned photolithographically, and the unwanted sections of lead removed by ion beam etching. In this last step a low current density ( $\sim 10^{-7}$  A/cm<sup>2</sup>) of the ion beam, resulting in slow, gentle, etching was found to be essential. Attempts to sputter etch the arrays, with ion current densities of the order of  $10^{-4}$  A/cm<sup>2</sup> resulted always in noticeable heating during the etching process, with deleterious effects on the quality of the S-N contact.

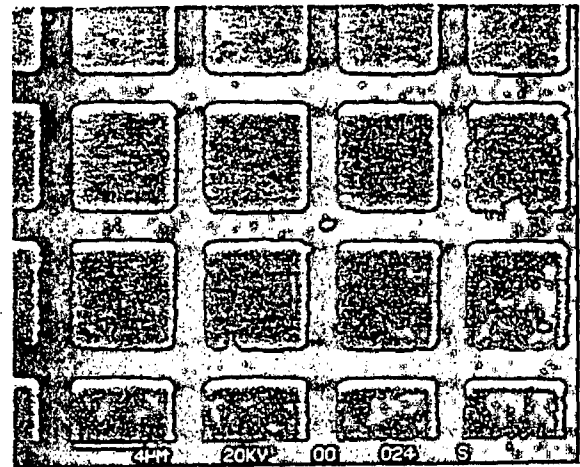


Figure 1. Scanning electron micrograph of a square array of lead islands on a copper film.

3. The Vortex Dielectric Constant

Since vortices interact logarithmically with each other, like the charges in a 2D Coulomb gas<sup>16</sup>, their response to a driving oscillating force field of angular frequency  $\omega$  is conveniently described in terms of a complex dielectric constant  $\epsilon(\omega, T)$ . In the dynamic theory for the KT transition developed by Ambegaokar et al<sup>18</sup>, both bound pairs of vortices and free vortex excitations contribute to  $\epsilon(\omega, T)$ . The contribution of bound pairs is determined by a characteristic length:

$$r_\omega = (14D/\omega)^{1/2} \quad (1)$$

where  $D = (c/\phi_0)^2 a^2 r_n k_B T$  is the vortex diffusion constant ( $r_n$  is the normal state resistance of an individual junction in the array). For a given frequency  $\omega$ , pairs of size larger than  $r_\omega$  do not respond.

The free vortex contribution is proportional to the free vortex areal density  $n_f$ , which in turn is proportional to  $\zeta_+(T)^{-2}$ , the free vortex correlation length above  $T_c$ . The unusual temperature dependence of  $\zeta_+(T)$  is a characteristic trait of the KT transition:

$$\zeta_+(\tilde{T}) = ac \exp[b(\tilde{T}-\tilde{T}_c)^{-1/2}]. \quad (2)$$

In this expression  $\tilde{T} = 2ek_B T/hj_c(T)$  is a dimensionless temperature parameter,  $i_c(T)$  is the critical current of a single junction of the array in the absence of thermal fluctuations<sup>19</sup>, and  $b$  and  $c$  are non-universal constants of order unity.

At low temperatures the response is dominated by bound pairs. At a temperature  $T_\omega > T_c$  defined by:

$$r_\omega \approx \zeta_+(T_\omega) \quad (3)$$

pairs of size  $r_\omega$  unbind. The response at temperatures  $T > T_\omega$  is thus dominated by the free vortices. Calculations based on these ideas<sup>18,20</sup> show that the real part of  $\epsilon^{-1}(\omega, T)$  is expected to drop from its low temperature value ( $1-\tilde{T}/4$ ) to 0 in the vicinity of  $T_\omega$ , while the imaginary part of  $\epsilon^{-1}(\omega, T)$  reaches a maximum close to  $T_\omega$  and vanishes both at low and at high temperatures. A strong theoretical prediction of the KT-theory is that the ratio

$$i_c(T_c) / \epsilon_c T_c = 8ek_B/h = 27 \text{ nA/K}, \quad (4)$$

where  $\epsilon_c$  is the value of the dielectric constant for a pair of infinite size, at  $T_c$ .

In order to measure the complex dielectric constant  $\epsilon(\omega, T)$  of 2D arrays, we have used a mutual inductance technique. Two concentric cylindrical coils, an external drive coil and an internal astatic pair receive coil, were placed directly on the sample. An ac current of amplitude  $I_0$  and angular frequency  $\omega$  flowing through the drive coil induces currents in the array which, in turn, induce a signal voltage  $\delta V_\omega$  in the receive coil. This voltage, which describes the screening properties of the array, can be written in the form<sup>21</sup>:

$$\delta V_\omega = -\omega^2 I_0 C(T) G(\omega, T), \quad (5)$$

where  $G(\omega, T)$  is the complex sheet conductance of the array. If normal currents flowing in the array can be neglected, i.e. if  $\omega L_K \ll r_n$ , where  $L_K(T) = \pi/2ei(T)$  is the bare sheet kinetic inductance of the array<sup>19</sup>, the sheet impedance  $Z(\omega, T)$  can be written as<sup>16</sup>:

$$Z(\omega, T) = i\omega L_K \epsilon(\omega, T). \quad (6)$$

In our arrays  $r_n$  is of the order of a few  $m\Omega$ , ( $r_n = 4 \text{ m}\Omega$  for the array studied in this work), so that Eq. (6) is valid at frequencies of up to some  $10^4$  Hz. As for the "coupling parameter"  $C(T)$  entering Eq. (5), a calculation similar to that reported in Ref. 21 and incorporating our coil-sample geometrical configuration yields, using Eq. (6):

$$C(T) = \int e^{-x} f(x) [x + (H/\Lambda(T)) \epsilon^{-1}(\omega, T)]^{-1} dx \quad (7)$$

where  $\Lambda(T) = (c\phi_0/4\pi^2)/i_c(T)$  is the bare transverse penetration depth of the array,  $H \approx 0.3 \text{ mm}$  is the distance of the first winding of the drive coil from the array and  $f(x)$  is an oscillating, damped function of  $x$  such that  $f(0) = 0$ , decaying as  $1/x$  at large  $x$  and depending only on the geometrical parameters of the coil system.

Expression (5) for  $\delta V_\omega$  reduces to a particularly simple form in the weak screening limit,  $\Lambda/H \gg 1$ . For

$\Lambda/H \gg 1$ , a condition satisfied by our arrays in the critical region around  $T_c$  ( $\Lambda(T_c) T_c = 1.96 \text{ cmK}^{19}$ ),  $C(T)$  turns out to be independent of  $T$ , the measured  $\delta V_\omega$  is directly proportional to  $Z^{-1}(\omega, T)$  and consequently (Eq. (6)), to  $\epsilon^{-1}(\omega, T)$ . The expected qualitative temperature dependence of  $\epsilon^{-1}(\omega, T)$  is thus already apparent in Fig. 2(a), where the real and imaginary parts of the measured signal as a function of temperature at a measuring frequency of 2156 Hz are shown for  $f = 0$ . From these data and Eqs. (5) and (7) it is possible, using an iterative procedure to extract the real and imaginary parts of  $\epsilon^{-1}(\omega, T)$  as a function of temperature. The result is shown in Fig. 2(b). In this calculation, there is only one adjustable parameter: the distance  $d$  between two successive windings of the detection coil, which was adjusted to yield  $\text{Re}[\epsilon^{-1}(\omega, T)] = 1$  at low temperatures. The resulting value,  $d \approx 32 \mu\text{m}$ , is consistent with the nominal wire diameter of  $20 \mu\text{m}$ .

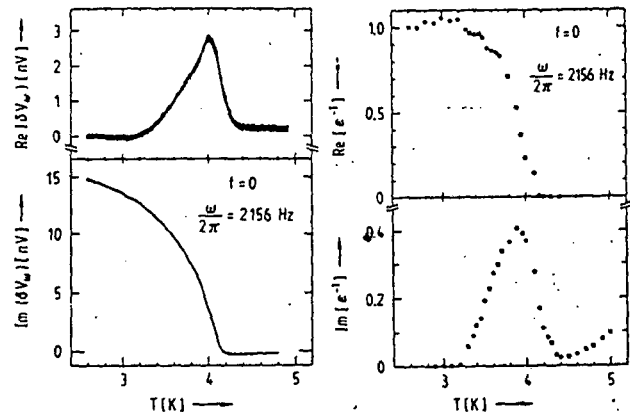


Figure 2. (a) Temperature dependence of the complex ac response of an array in zero magnetic field ( $f = 0$ ). (b) Inverse vortex dielectric constant as a function of temperature, extracted from the data of Fig 2 (a).

The single junction critical currents,  $i_c(T)$  necessary to evaluate  $\Lambda(T)$ ,  $L_K(T)$  and, for the scaling analysis of the following section,  $\tilde{T}$ , were obtained from low temperature measurements of the array's critical current. These measurements were found to fit the expression<sup>12,22</sup>

$$i_c = i_0 (1-T/T_{CS})^2 \exp[-L/\zeta_n(T)]. \quad (8)$$

extremely well, with a measured BCS transition temperature of the Pb islands  $T_{CS} = 6.8 \text{ K}$  and fit parameters  $\zeta_n(T_{CS}) = 10^3 \text{ \AA}$  for the Cu coherence length and  $i_0 = 0.129 \text{ \AA}$ . The large ratio  $L/\zeta_n = 17$  guarantees a sinusoidal current-phase relation<sup>23</sup>, justifying the description of the array with an XY-model.

#### 4. The Unfrustrated Array ( $f = 0$ )

A comparison of the results of Fig. 2(b) with the theoretical curves calculated from the KT scaling equations<sup>2</sup> shows that, while the  $\text{Re}[\epsilon^{-1}]$  vs.  $T$  data exhibit a good quantitative agreement, the peak in the experimental  $\text{Im}[\epsilon^{-1}]$  vs  $T$  curve is much wider than the theoretically expected one. In fact, whereas the theoretical width for a scale  $l_\omega = \ln(r_\omega/a) \approx 2$  at 2156 Hz is about .2K, the experimental peak is about 1 K wide. Although the origin of this anomaly is not totally understood at present, it seems plausible to attribute it to vortex unbinding induced by the driving ac current. In fact with increasing amplitude of the measuring current, the width of the peak in  $\text{Im}[\epsilon^{-1}(T)]$  is

found to increase, while its position shifts to lower temperatures. This observation indicates that non-linear effects associated with finite driving currents are at least partially responsible. The relationship between the current flowing in the excitation coil and the position of the peak in the  $\text{Re}(\delta V_\omega)$  vs  $T$  curve is shown in Fig. 3 for two measuring frequencies.

As predicted by Eqs.(2) and (3), with increasing measuring frequency the structures in the measured  $\delta V_\omega$  vs  $T$  curves should shift to higher temperatures. This is observed in our experiments<sup>17</sup> and, if some way of determining  $T_\omega$  from the data is found, the temperature dependence of the free vortex correlation length above  $T_C$  can be deduced from the measurements of  $\delta V_\omega(T)$  performed at different frequencies. We define  $T_\omega$  by extrapolating to zero the linear sections of the  $\text{Im}(\delta V_\omega)$  vs  $T$  curves. As is obvious from Fig. 3, defining  $T_\omega$  as the temperature corresponding to the peak in  $\text{Re}(\delta V_\omega(T))$ <sup>20</sup> depends on the measuring current  $I_D$ . However, if the straight lines in Fig. 3 are extrapolated to zero measuring current, we find that the resulting  $T_\omega$  is within 5mK of the value obtained by extrapolating the  $\text{Im}(\delta V_\omega)$  vs  $T$  curves as described above.

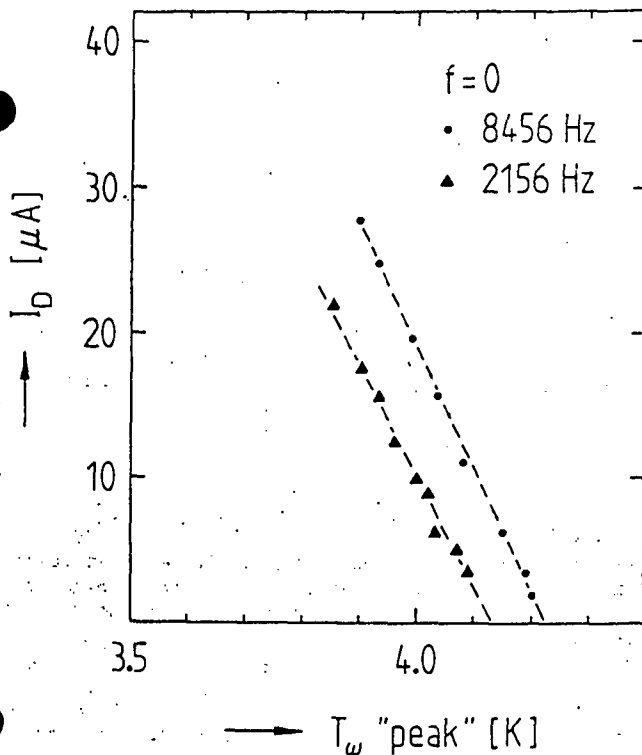


Figure 3. Position of the "peak" temperature as a function of driving current for two different frequencies, 2156 Hz and 8456 Hz in zero field. The extrapolation to zero driving current defines  $T_\omega$ .

With the scale parameter  $l_\omega$  defined above, Eq. (2) can be written as :

$$l_\omega = b(\tilde{T}_\omega - \tilde{T}_C)^{-1/2} + \ln c \quad (8)$$

A plot of  $l_\omega$  vs  $\tilde{T}$  is shown in Fig. 4, together with a fitted curve with parameter values  $\tilde{T}_C = 0.77 \pm 0.02$ ,  $b = 1.39 \pm 0.14$  and  $c = 0.61 \pm 0.1$ . This clearly demonstrates that the temperature dependence of the free vortex correlation length has the exponential inverse square-root form. From our experimental value of  $\tilde{T}_C = 0.77$  we obtain a ratio  $i_C(\tilde{T}_C)/T_C = 54$  nA/K. Inserting this result in the universal prediction given by Eq. (4) gives  $\epsilon_C = 2.04$ , a value in good agreement with an estimate ( $\epsilon_C = 1.75$ ) obtained from a Monte Carlo simulation of the X-Y model<sup>3,4</sup>.

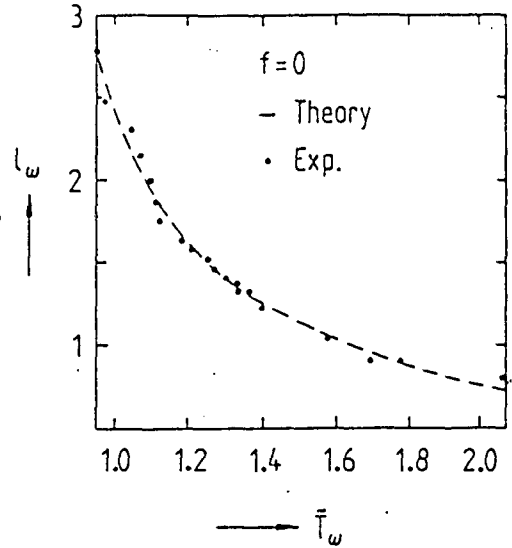


Figure 4. Dependence of the scale parameter  $l_\omega = \ln(r_\omega/a)$  (where  $a$  is the lattice constant) on the reduced temperature  $T_\omega$ , confirming the theoretically predicted (dashed line, Eq. 8) temperature dependence of the free vortex correlation length above  $T_C$ .

### 5. Frustration Effects

The magnetic field dependence of the ac response has also been investigated<sup>7</sup>. Real and imaginary parts of the signal voltage  $\delta V_\omega$  as a function of the frustration parameter  $f$  are shown in Fig.5. These  $\delta V_\omega$  vs  $f$  curves were taken at a temperature of 2.91 K, well below the normal-superconducting phase boundary  $T_C(f)$ , where the influence of thermally activated topological excitations of various kind (vortices, domain wall, dislocations) is negligible. Sharp structures emerge in both the real and imaginary components of  $\delta V_\omega$  in correspondence to commensurate (C) vortex phases defined, in the range  $0 < f < 1/2$ , by the rational values 0, 1/3 and 1/2 of the frustration parameter  $f$ . The symmetry of the "fine structure" about  $f = 0$  in the  $\delta V_\omega$  vs  $f$  curves shows that C-phases of higher order have also been resolved. Except for the quadratic background, due to the finite size of the individual junctions, the structures in  $\delta V_\omega(f)$  are periodic in  $f$  with period 1 and their relative strength qualitatively agrees with predictions of the "staircase" model<sup>10</sup> and of Monte Carlo simulations<sup>7,8</sup>. At low temperatures ( $T \ll T_C(f)$ ) the characteristic shape of the commensurate structures in  $\delta V_\omega(f)$  at rational values of the frustration parameter can be explained in terms of the interaction of the lattice of field-induced vortices with the periodic potential provided by the array. In a low order C-phase the mobility of the vortices is considerably reduced by the periodic potential, while the vortex lattice can slide freely in an incommensurate phase. As a consequence, in a low order C-phase there is a marked reduction of dissipation, a process resulting in the pronounced commensurate dips one observes in the  $\text{Re}(\delta V_\omega(f))$  signals of Fig. 5. At the same time considerable lag in response is expected for such vortex configurations. This mechanism is obviously at the origin of the commensurate peaks in the inductive component,  $\text{Im}(\delta V_\omega(f))$ , of the signals.

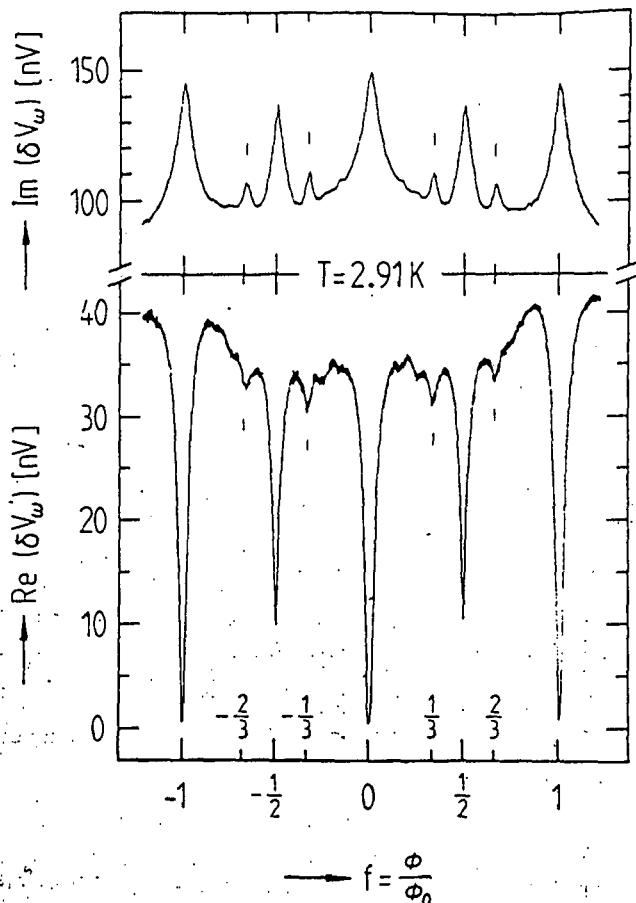


Figure 5. Real and imaginary parts of the array's response  $\delta V_\omega$  as a function of the frustration parameter  $f = Ba^2/\Phi_0$  at a temperature  $T = 2.91K$ . The structures observed at rational  $f$  values correspond to commensurate phases of the field induced vortex lattice with the periodic pinning potential provided by the array.

## 6. Conclusions

Our dynamical method allows us to probe the vortex medium at different scales, thereby providing an extremely sensitive detector for studying the nature of the phase transition in 2D arrays and their magnetic field properties.

For  $f$  integer we have shown that the dynamics of the topological defects has features allowing their identification as the vortex excitations of the KT-theory. For a frustrated array more work is needed to ascertain the nature of the topological excitations and their possible role in triggering the phase transition at  $T_c(f)$ .

We thank M. F. Pressel-Wenger for taking the SEM picture. This work was supported by the Fond National Suisse pour la Recherche Scientifique.

## References

1. J.E. Mooij, in: Percolation, Localization and Superconductivity, ed. by A.M. Goldman and S.A. Wolf, NATO ASI Series B: Phys. Vol. 109 (Plenum, New-York 1984)
2. J.M. Kosterlitz and D.J. Thouless, *J. Phys.* **C6**, 1181, 1973
3. D.J. Resnick, J.C. Garland, J.T. Boyds, S. Shoemaker and R.S. Newrock, *Phys. Rev. Lett.* **47**, 1542, 1981
4. D.W. Abraham, C.J. Lobb, M. Tinkham and T.M. Klapwijk, *Phys. Rev.* **B26**, 5268, 1982
5. D. Kimhi, F. Leyvraz and D. Ariosa, *Phys. Rev.* **B29**, 1487, 1984
6. R.A. Webb, R.F. Voss, G. Grinstein and P.M. Horn, *Phys. Rev. Lett.* **51**, 690, 1983
7. S. Teitel and C. Jayaprakash, *Phys. Rev. Lett.* **51**, 1999, (1983), and *Phys. Rev.* **B27**, 598, 1983
8. W.Y. Shih and D. Stroud, *Phys. Rev. B* **28**, 6575, 1983 and **30**, 6774, 1984 and **32**, 158, 1985
9. M.Y. Choi and S. Doniach, *Phys. Rev.* **B31**, 4516, 1985
10. T.C. Halsey, *Phys. Rev.* **B31**, 5728, 1985 and *Phys. Rev. Lett.* **55**, 1018, 1985
11. D.H. Lee, J.D. Joannopoulos, J.W. Negele and D.R. Landau, *Phys. Rev. Lett.* **52**, 433, 1984 and *Phys. Rev.* **B33**, 450, 1986
12. M. Tinkham, D.W. Abraham and C.J. Lobb, *Phys. Rev.* **B28**, 6578, 1983
13. V.S. Dotsenko and G.V. Uimin, *J. Phys.* **C18**, 5019, 1985
14. M. Yosefin and E. Domany, *Phys. Rev.* **B32**, 1778, 1985
15. E. Granato and J.M. Kosterlitz, *Phys. Rev.* **B33**, 4767, 1986
16. A.F. Hebard and A.T. Fiory, *Phys. Rev. Lett.* **44**, 291, 1980 and *Physica (Amsterdam)* **109&110 B+C**, 1637, 1982
17. Ch. Leemann, Ph. Lerch, G.A. Racina and P. Martinoli, *Phys. Rev. Lett.* **56**, 1291, 1986
18. V. Ambegaokar, B.I. Halperin, D.R. Nelson and E.D. Siggia, *Phys. Rev. Lett.* **40**, 783, 1978 and *Phys. Rev.* **B21**, 1806, 1980
19. C.J. Lobb, D.W. Abraham and M. Tinkham, *Phys. Rev.* **B27**, 150, 1983
20. S.R. Shenoy, *J. Phys. C* **18**, 5163, 1985
21. A.T. Fiory and A.F. Hebard in: Inhomogeneous Superconductors, ed. by D.U. Gubser, T.L. Francavilla, S.A. Wolf and J.R. Leibowitz, AIP Conference Proceedings No 58 (American Institute of Physics, New-York 1980) p.293
22. P.G. De Gennes, *Rev. Mod. Phys.* **36**, 255, 1964
23. K. Likharev, *Rev. Mod. Phys.* **51**, 101, 1979
24. J. Tobochnik and G.V. Chester, *Phys. Rev.* **B20**, 3761, 1979

Proc. 18th Int. Conf. on Low Temperature Physics, Kyoto, 1987  
Japanese Journal of Applied Physics, Vol. 26 (1987) Supplement 26-3

## **Arrays of Josephson Junctions: Model Systems for Two-Dimensional Physics**

P. MARTINOLI, Ph. LERCH, Ch. LEEMANN, and H. BECK

Institut de Physique, Université de Neuchâtel, CH-2000 Neuchâtel, Switzerland

## Arrays of Josephson Junctions: Model Systems for Two-Dimensional Physics

P. MARTINOLI, Ph. LERCH, Ch. LEEMANN, and H. BECK

Institut de Physique, Université de Neuchâtel, CH-2000 Neuchâtel, Switzerland

Planar arrays of Josephson junctions provide excellent model systems to study a variety of phase transitions in two dimensions. Experiments are reported in which the critical behaviour of periodic arrays is studied by measuring the dynamic response of the system to a small oscillating field. Tuning of frustration occurs by adjusting the magnetic flux threading a unit cell of the array, while by varying the driving frequency it is possible to probe the critical behaviour of the system at different length scales. The dynamic response near the phase transition of an unfrustrated array is well described by a model incorporating the vortex unbinding mechanism predicted by the Kosterlitz-Thouless theory. Some aspects of the dynamic response of frustrated arrays are also discussed.

### 1. INTRODUCTION

Renormalization, scaling, frustration, commensurability and randomness are essential concepts for the understanding of fundamental phenomena occurring in physics, biology and other areas of science. In this context, arrays of Josephson junctions [1-9] and superconducting wire networks [10-14] with structures ranging from periodic to random patterns and including quasiperiodic and fractal configurations provide model systems where the validity and the consequences of all these ideas can be explored, under nearly ideal conditions, in two dimensions.

Two-dimensional (2D) arrays of identical weak links with a sinusoidal current-phase relation exposed to a perpendicular magnetic field  $\vec{B}$  are described by the Hamiltonian [15-17] :

$$H = [\hbar i_c(T)/2e] \sum_{\langle ij \rangle} [1 - \cos(\phi_i - \phi_j - A_{ij})] \quad , \quad (1)$$

where  $\phi_i$  is the phase of the order parameter,  $\phi_i = |\phi_i| \exp(i\phi_i)$ , in the superconducting node at the site  $i$ ,  $A_{ij}$  is a bond variable proportional to the line integral of the vector potential  $\vec{A}$  across the link  $\langle ij \rangle$ ,  $A_{ij} = (2\pi/\Phi_0) \int_1^j \vec{A} \cdot d\vec{s}$ , and  $i_c(T)$  is the critical current of an isolated junction of the array in the absence of thermal fluctuations. If one identifies  $\phi_i$  with the angle between a planar classical spin at the site  $i$  and a fixed arbitrary direction in the lattice plane, then Eq. (1) shows that periodic 2D Josephson junction arrays in a magnetic field are isomorphic to a frustrated XY model with a temperature-dependent coupling energy  $J(T) = \hbar i_c(T)/2e$ . The degree of frustration is controlled by the ratio  $f = \Phi/\Phi_0$  expressing the magnetic flux  $\Phi$  per unit cell in units of the superconducting flux quantum  $\Phi_0$  and satisfying the condition  $\sum_{\langle ij \rangle} A_{ij} = 2\pi f$ , where the sum is over the links  $\langle ij \rangle$  in a unit cell. Because of the temperature dependence of  $J$ , the statistical mechanics of the system is conveniently described in terms of a dimensionless temperature parameter  $\bar{T} = [k_B T/J(T)]$  [15].

The critical behaviour of a 2D periodic array of Josephson junctions has been studied in a number of theoretical papers using renormalization-group [18-24] and mean-field [25] methods, Monte Carlo simulations [17, 25-29] and symmetry analysis [27, 30-32]. For the unfrustrated system ( $f$  integer) the Kosterlitz-Thouless (KT) theory [18] predicts, at a critical temperature  $T_C$ , a transition from a superconducting state ( $\bar{T} < T_C$ ) with

quasi long-range (or topological) order in the phases  $\{\phi_i\}$  to a normal state ( $\bar{T} > T_C$ ) with liquid-like disorder in the  $\{\phi_i\}$ . The phase transition at  $T_C$  is attributed to the unbinding of vortex-antivortex pairs resulting from 2D thermal fluctuations in the  $\{\phi_i\}$ . Experiments [1-4, 6, 7, 9, 14] tend to support the KT vortex unbinding idea. The physics of frustrated arrays ( $f$  non-integer) is more complex and only partially understood at present. Although solutions for the ground-state ( $\bar{T} = 0$ )  $\phi_i$ -pattern have been found for a few rational values of  $f$  [30], detailed theoretical predictions concerning the nature of the phase transition at  $T_C(f)$  exist only for the fully frustrated array ( $f$  half-integer in a square lattice). In this case the presence of both vortex and domain-wall excitations [17, 27, 30-32] should lead to a single transition with mixed KT and Ising-like features [21-24, 27, 28, 30, 32]. This double nature is difficult to observe experimentally, although recent results [9] suggest a critical behaviour different from that predicted by the KT theory.

In a recent Letter [7] we reported experiments in which the critical behaviour of 2D arrays of proximity-effect coupled Josephson junctions was studied by measuring the dynamic response of the array to a small oscillating field. In the ac response of the unfrustrated system we found features providing strong evidence for a phase transition driven by the vortex unbinding mechanism predicted by the KT theory. In this paper we give a fairly complete theoretical description of the dynamics of unfrustrated arrays in the critical region (Sec. 2). The model provides the background for a detailed theoretical interpretation of our earlier experiments (Sec. 3). Some aspects of the dynamic response of frustrated arrays, in particular of the fully-frustrated system, are discussed in Sec. 4.

### 2. PHASE AND VORTEX DYNAMICS

To study the dynamic response of a 2D array to a small time-dependent excitation, we rely on a time-dependent Ginzburg-Landau (TDGL) approach [33]. Since only phase fluctuations are expected to be important in the critical region near  $T_C(f)$ , from the TDGL equation describing order parameter relaxation we deduce the following gauge-invariant equation for  $\phi_i(t)$  :

$$\hbar \frac{\partial \phi_i}{\partial t} - 2\mu_i = -\gamma \frac{\partial H}{\partial \phi_i} \quad , \quad (2)$$

where  $\mu_i$  is the electrochemical potential in the superconducting island at the site  $i$  and  $H$  is given by Eq. (1). Assuming a RSJ-model [34] for an individual junction of the array, we expect the characteristic time  $\tau_0 = \hbar/\gamma J$  which governs the phase relaxation process to be given by  $\tau_0 = \hbar/2ei_c r_n$ , where  $r_n$  is the normal-state resistance of a single junction. To deal with a tractable problem, we replace the cosine-term in Eq. (1) with a piecewise parabolic potential  $U(\theta_{ij})$  :

$$U(\theta_{ij}) = (1/2) \sum_n \chi(\theta_{ij}-n\pi)(\theta_{ij}-2n\pi)^2 - 1, \quad (3)$$

where  $\theta_{ij} = \phi_i - \phi_j - A_{ij}$ ,  $n$  is an integer labelling the parabolic wells and  $\chi(u)$  is such that  $\chi(u) = 1$  for  $|u| \leq 1$  and vanishes otherwise. To establish a closer connection with our experiments, we seek an equation for the current circulating in the array rather than for  $\phi_i(t)$ . Accordingly, within the model based on (3) we define the Josephson current  $I_{ij}$  flowing through the junction  $\langle ij \rangle$  by  $I_{ij} = i_c \partial U / \partial \theta_{ij} = i_c [\theta_{ij} + Q(\theta_{ij})]$ , where  $Q(\theta_{ij}) = -2\pi \sum_n \chi(\theta_{ij}-n\pi)n$  is a staircase function of  $\theta_{ij}$  with discontinuous jumps of  $-2\pi$  at  $(2n+1)\pi$ . Thus,  $I_{ij}$  is a sawtooth function of  $\theta_{ij}$ . Writing the total vector potential as a sum of a static contribution,  $\vec{A}$ , corresponding to  $\vec{B}$  and of a time-dependent term,  $\vec{a}(t)$ , due to a weak driving field, to lowest order in  $\vec{a}(t)$  the equation for  $I_{ij}(t)$  following from Eqs. (1)-(3) reads :

$$L_{K\Box} \frac{\partial I_{ij}}{\partial t} = -r_n \sum_s (I_{is} - I_{js}) + \frac{\hbar}{2e} \frac{\partial Q(\theta_{ij})}{\partial t} + V_{ij}(t), \quad (4)$$

where  $L_{K\Box} = \hbar/2ei_c$  is the (bare) sheet kinetic inductance of the array,  $V_{ij}(t) = (1/e)(\mu_i - \mu_j) - \int_1^j (\partial \vec{a} / \partial t) \cdot d\vec{s}$  is the potential difference across the link  $\langle ij \rangle$  [35] and the sum is over the nearest-neighbours (4 in a square lattice) of the sites  $i$  and  $j$ . From Eq. (4) we see that the effect of frustration enters the problem through the quantity  $Q(\theta_{ij})$ . As a consequence, we expect the  $Q(\theta_{ij})$ -term in Eq. (4) to describe the dynamics of those topological excitations which, from symmetry considerations [30-32], are known to be relevant for the critical behaviour of a frustrated array. For arbitrary frustration, a theory linking the motion of topological excitations of various kinds (vortices, domain walls, dislocations) to  $Q(\theta_{ij})$  is not available so far. For the unfrustrated system, however,  $Q(\theta_{ij})$  can be easily related to vortex motion. To show this explicitly, we introduce an areal vortex density  $n_v$  and a 2D vortex current density  $\vec{K}_v$  which satisfy the continuity equation,  $\dot{n}_v + \nabla \cdot \vec{K}_v = 0$ , for vortex conservation [36]. Since the length scales probed in experiments are usually much larger than the lattice spacing, in the unfrustrated case we can ignore the effect of lattice discreteness and take a continuum approximation. In this limit  $Q[\phi_i(t) - \phi_j(t)]$  can be expressed in terms of a vector  $\vec{Q}(\vec{r}, t)$ . Then,  $n_v$  and  $\vec{K}_v$  are related to  $\vec{Q}$  by [36,37] :

$$\nabla \times \vec{Q} = 2\pi n_v \hat{z}, \quad \frac{\partial \vec{Q}}{\partial t} = -2\pi (\hat{z} \times \vec{K}_v), \quad (5)$$

where  $\hat{z}$  is a unit vector normal to the array. These relations show quite clearly that  $\vec{Q}$  is proportional to the superfluid velocity associated

with the vortex field. Using Eq. (5), the equation of motion (4) for the unfrustrated system becomes, in the continuum approximation :

$$\vec{E} = L_{K\Box} \frac{\partial \vec{K}_s}{\partial t} - r_n d^2 \nabla (\nabla \cdot \vec{K}_s) + \Phi_0 (\hat{z} \times \vec{K}_v), \quad (6)$$

where  $\vec{K}_s$  is the sheet supercurrent density flowing in the array and  $d$  the lattice spacing. As for 2D superconducting films [36], Eq. (6) reveals the decomposition of the driving electric field  $\vec{E}$  into contributions from the superfluid background [with an additional term,  $\nabla (\nabla \cdot \vec{K}_s)$ , resulting from spin-wave-like excitations of the phase] and vortex excitations.

To proceed further in our study of the dynamic response of unfrustrated arrays, we need a relation between  $\vec{K}_v$  and  $\vec{K}_s$ . In a phenomenological model of the vortex medium based on a 2D Coulomb-gas analogue [36], dynamical screening is described in terms of a complex vortex dielectric constant  $\epsilon(T, \omega)$ , which is a sum of a contribution  $\epsilon_b(T, \omega)$  from vortex-antivortex dipoles and  $2\pi\sigma_v(T)/i\omega$  from free vortex charges :

$$\epsilon(T, \omega) = \epsilon_b(T, \omega) + [2\pi\sigma_v(T)/i\omega], \quad (7)$$

where  $\sigma_v(T)$  is the free-vortex conductivity [38]. Relying on the 2D Coulomb-gas analogy, the  $\vec{K}_v - \vec{K}_s$  relation, written in terms of Fourier-transformed quantities, turns out to be :

$$\Phi_0 (\hat{z} \times \vec{K}_v) = i\omega L_{K\Box} [\epsilon_b - 1 + (2\pi\sigma_v/i\omega)] \vec{K}_s. \quad (8)$$

The vortex dielectric constant  $\epsilon(T, \omega)$  has been calculated in dynamical extensions of the KT theory [39-41]. The complex bound pair contribution  $\epsilon_b(T, \omega)$  can be expressed in terms of the scale- and temperature-dependent dielectric constant  $\epsilon(\lambda, T)$  of the static KT theory [ $\lambda = \lambda n(r/d)$  is the reduced scale]. According to the dynamical theory [39-41], experiments performed at finite frequencies select out a characteristic length  $r_\omega \approx (14D/\omega)^{1/2}$ , where  $D$  is the vortex diffusivity, representing the size of those vortex-antivortex pairs which dominate the response. Then, the theoretical prediction for  $\text{Re}[\epsilon_b(T, \omega)]$ , the quantity which can be most easily extracted from the experiments presented in Sec. 3, is simply :

$$\text{Re}[\epsilon_b(T, \omega)] = \epsilon(\lambda_\omega, T), \quad (9)$$

where  $\lambda_\omega = \lambda n(r_\omega/d)$ . From an expression of  $D$  appropriate to arrays [7,38], we obtain  $2\lambda_\omega = \lambda n(14r_n k_B T / \Phi_0^2 \omega)$ .  $\epsilon(\lambda_\omega, T)$  follows from a numerical integration of the Kosterlitz scaling equations [42,43]. In this connection, we notice that spin-wave fluctuations are usually ignored in the analysis of 2D superconducting systems. According to Minnhagen [29], however, the influence of spin-wave excitations can be approximately incorporated in the KT theory using, instead of  $T$ , an effective Coulomb-gas temperature  $\tau$  in the scaling equations. For an unfrustrated array  $\tau$  and  $T$  are related by  $\tau = T / [1 - (T/4)]$  [29]. We shall adopt Minnhagen's approach in the analysis of the next section.

### 3. PHASE TRANSITION AT ZERO FRUSTRATION

We have studied the complex ac response of 2D arrays of proximity-effect Pb/Cu/Pb junctions and of Al-wire networks using a two-coil mutual-inductance technique [7,36,38]. The experiments reported here were performed on an array consisting of  $N \times N \approx 10^6$  square Pb islands forming a square lattice with  $d = 8 \mu\text{m}$  on a Cu layer. An individual junction of the array has  $r_n = 4m\Omega$ . The  $i_c(T)$  curve needed for the analysis of the data was obtained by fitting low-temperature  $i_c$ -measurements to the expression  $i_c(T) = i_0[1-(T/T_{CS})]^2 \exp[-L/\xi_n(T)]$ , using  $i_0 = 0.129 \text{ A}$ ,  $T_{CS} = 6.8 \text{ K}$  for the BCS transition temperature of the Pb islands,  $\xi_n(T_{CS}) = 1130 \text{ \AA}$  for the Cu coherence length and  $L = 1.7 \mu\text{m}$  for the length of the Cu bridges connecting adjacent Pb islands [16]. The Al-network consists of wires of width  $1.4 \mu\text{m}$  forming a square lattice of  $\sim 10^6$  nodes with  $d = 8 \mu\text{m}$  and strip resistance  $R_S = 95 \Omega$  [14].

The signal voltage  $\delta V_\omega$  at the receiving coil due to the screening currents circulating in the array in response to an ac current  $I_{D\omega}$  flowing in the driving coil is related to the complex sheet impedance  $Z_\square$  of the sample by [7,38] :

$$\delta V_\omega = \omega^2 I_{D\omega} f(Z_\square) \quad (10)$$

If screening is weak,  $f(Z_\square)$  is proportional to the sheet conductance  $G_\square = Z_\square^{-1}$  of the array. This condition is satisfied at all temperatures of interest in the Al-network but only in the immediate vicinity of  $T_C$  in the proximity-effect array. In this system screening effects are important at lower temperatures where  $f(Z_\square)$  becomes independent of  $Z_\square$  [38]. If we define  $Z_\square$  by  $\tilde{\epsilon} = Z_\square \tilde{\kappa}_S$ , then from Eqs. (6)-(8) we obtain :

$$Z_\square(T, \omega) = i\omega L \tilde{\kappa}_\square(T) \epsilon(T, \omega) \quad (11)$$

In deriving this expression we have ignored the  $\nabla(\nabla \cdot \tilde{\kappa}_S)$ -term in Eq.(6), whose contribution is negligible at the typical frequencies and wave vectors  $\tilde{q}$  of our experiments [ $(\tilde{q}d)^2 \ll \omega\tau_0$ ]. From Eqs. (10) and (11) it follows that, near  $T_C$ ,  $\delta V_\omega$  is proportional to  $i_c(T)/\epsilon(T, \omega)$ . Since  $i_c(T)$  is a monotonic function of temperature, measurements of  $\delta V_\omega$  in the critical region around  $T_C$  should mostly reflect the behaviour of  $\epsilon^{-1}(T, \omega)$ , for which dynamical extensions of the KT theory [39-41] predict a drop in the real part (the superfluid component) and a peak in the imaginary part (the dissipative component). These characteristic features of the KT transition are present in the data of Fig. 1, where the complex ac response of the Pb/Cu/Pb array measured at 2.2 and 8.5 kHz is shown as a function of temperature. The onset of substantial screening effects below  $T_C$  partly masks the falloff in  $\text{Im}[\delta V_\omega(T)]$ , which shows up as a slight change in slope at about 3.95 K in the low-frequency data. As shown in Fig. 2, however, the structures in  $\epsilon^{-1}(T, \omega)$  predicted by the theory become quite manifest once the vortex dielectric constant is unfolded from the ac response given by Eq. (10) using an expression for  $f(Z_\square)$  appropriate for the sample-coil configuration of our experiments [38].

An additional feature of the results shown in Fig. 2 is worth mentioning : the long tail on the low-temperature side of the peak in  $\text{Re}[\delta V_\omega(T)]$ , which is found to be very sensitive to the amplitude of the small but non-vanishing driving current. We attribute this non-linear effect to cur-

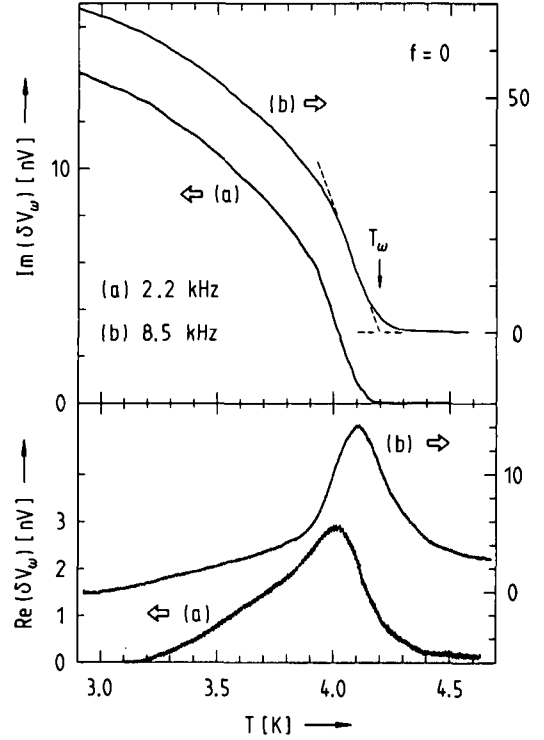


Fig. 1. Temperature dependence of the complex ac response of an unfrustrated 2D array of proximity-effect Josephson junctions at two different frequencies.

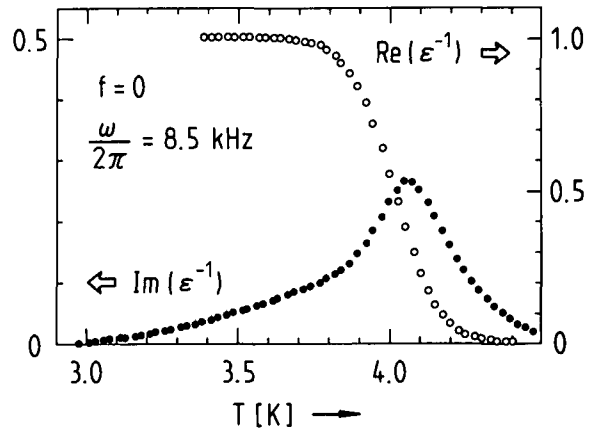


Fig. 2. Temperature dependence of the complex inverse vortex dielectric constant as deduced from the 8.5 kHz-data for the proximity-effect array of Fig. 1.

rent-induced vortex unbinding resulting in additional dissipation below  $T_C$  [39,40,43-45].

In wire networks with moderate strip resistance the vortex unbinding transition at  $T_C$  [17] is very close to the GL mean-field transition which occurs at a temperature  $T_{CO} > T_C$  [10,46,47]. Therefore, the KT transition is difficult to observe in purely resistive measurements. As shown above, however, measurements of the dynamic response in the weak screening limit couple directly

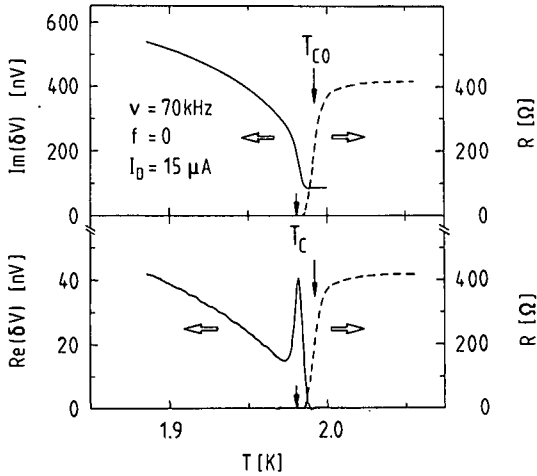


Fig. 3. Temperature dependence of the complex ac response and of the dc resistance in the critical region of an unfrustrated wire network.

to the *sheet conductance* of the system and are therefore very sensitive to the onset of dissipation due to the proliferation of free vortices. This is clearly demonstrated by the ac response at 70 kHz of the Al-network shown in Fig. 3, where the characteristic features of the KT transition are observed in a narrow temperature range *below*  $T_{CO}$ . A detailed analysis of these experiments is reported elsewhere in the proceedings of this conference [14].

Deeper insight into the nature of the phase transition is provided by a study of the temperature dependence of the helicity modulus,  $\Gamma$ , of the Pb/Cu/Pb array, a quantity which measures phase correlation in the system.  $\Gamma$  is related to the renormalized stiffness,  $K(\lambda, \tau) = [\epsilon(\lambda, \tau)\tau]^{-1}$  [43], by  $\Gamma = KT$  [19]. Thus,  $\Gamma$  can be written as :

$$\Gamma = [\epsilon(\lambda, \tau)]^{-1} [1 - (\tilde{T}/4)] \quad (12)$$

Since from Eqs.(7) and (9) we expect  $Re[\epsilon(T, \omega)] = \epsilon(\lambda_\omega, T)$ ,  $\Gamma$  can be easily extracted from the  $\epsilon$ -data of Fig. 2. The result is shown in Fig. 4, where  $\Gamma$  is plotted as a function of  $\tilde{T}$  along with a theoretical curve for  $\Gamma(\tilde{T})$  obtained by numerically integrating the Kosterlitz scaling equations for  $\lambda_\omega = 1.3$  [43]. In accordance with the theoretical prescription, the integration is truncated at a temperature  $T_\omega > T_C$  such that  $\lambda_\omega = \lambda_+$ , where  $\lambda[\xi_+(T)/d]$  is the reduced scale corresponding to the free-vortex correlation length  $\xi_+(T)$  above  $T_C$  [43]. The overall agreement is excellent, considering that all quantities needed for the analysis are measured with the exception of two adjustable parameters which are used to model the vortex core energy [43] :  $\epsilon_C$ , the vortex dielectric constant for infinite scale at  $T_C$  and  $N_0$ , a parameter related to the vortex configurational entropy. From the fit of Fig. 4 we deduce  $\epsilon_C = 1.69$  and  $N_0 = 0.25$ . The value of  $\epsilon_C$  is in reasonable agreement with that ( $\epsilon_C = 1.33$ ) inferred from Monte Carlo simulations [17] using the universal prediction  $\epsilon_C \tau_C = \pi/2$ .

Further evidence for the KT transition is found by studying the frequency dependence of the dynamical response [7]. As shown by the data of Fig. 1, the transition shifts to higher temperatures with increasing  $\omega$ . To explain this observation, we re-

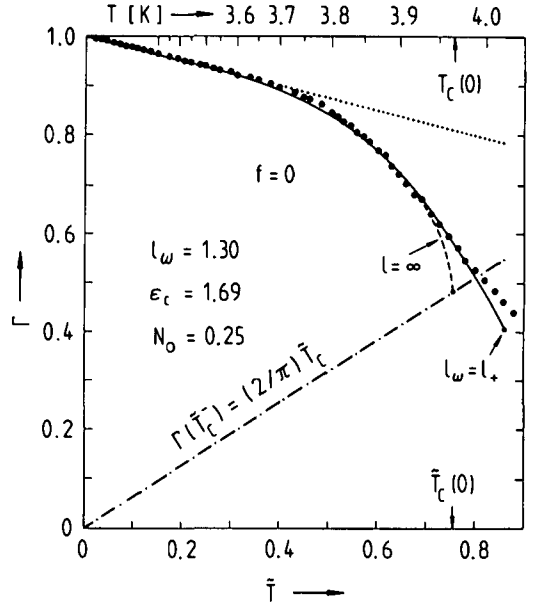


Fig. 4. Helicity modulus of the unfrustrated proximity-effect array of Fig. 1 as a function of the dimensionless temperature  $\tilde{T}$ . Full circles : Experimental results inferred from the  $\epsilon$ -data of Fig. 2. Solid curve : calculation based on the KT theory using the parameter values shown in the figure. The dotted dashed line is the KT universal-jump prediction. The dotted line is the low-temperature theoretical prediction based on spin waves only.

call that the dynamical theories [39-41] predict a crossover in response triggered by the unbinding of bound vortex pairs into free vortices at a temperature  $T_\omega$  such that  $r_\omega = \xi_+(\tau_\omega)$ . The correlation length  $\xi_+(\tau)$  has an exponential inverse square-root temperature dependence :  $\xi_+(\tau) \approx \text{dexp}[b(\tau - \tau_C)^{-1/2}]$ , where  $b$  is a constant of order unity [18,43]. As shown in Fig. 1, we define  $T_\omega$  by extrapolating to zero the steep portion of the superfluid component,  $Im[\delta V_\omega(T)]$ , of the response, a procedure independent of  $I_{D\omega}$  [7]. Using the scale parameter  $\lambda_\omega$ , the crossover condition  $r_\omega = \xi_+(\tau_\omega)$  becomes :

$$\lambda_\omega^{-2} = b^{-2} (\tau_\omega - \tau_C) \quad (13)$$

We plot  $\lambda_\omega^{-2}$  vs  $\tau_\omega$  in Fig. 5. A good fit to Eq. (13) is obtained for  $b = 1.31$  and  $\tau_C = 1.05$ . This value of  $b$  is in excellent agreement with that ( $b = 1.30$ ) calculated [43] using the values of  $\epsilon_C$  and  $N_0$  deduced from the analysis of  $\Gamma(\tilde{T})$  (Fig. 4). Furthermore, from the  $\tau_C$ -value and the universal prediction  $\epsilon_C \tau_C = \pi/2$  we obtain  $\epsilon_C = 1.50$ , which agrees reasonably with the value resulting from the fit of Fig. 4. The overall consistency emerging from our analysis of the temperature and frequency dependence of the response provides convincing evidence for the KT interpretation of the critical behaviour of unfrustrated arrays.

#### 4. FRUSTRATED ARRAYS

In arrays exposed to a perpendicular magnetic field  $\vec{B}$ , the interaction of the lattice of field-induced vortices with the pinning potential provi-

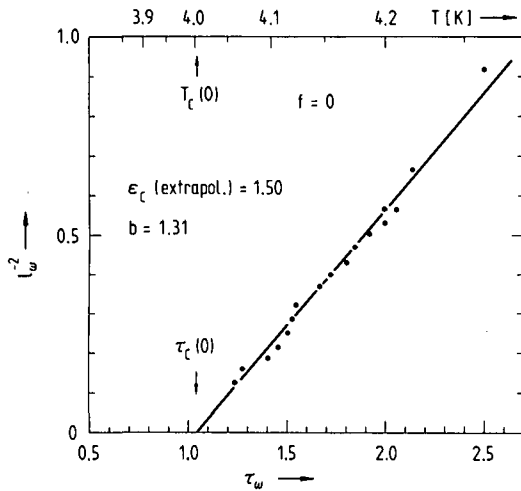


Fig. 5. Dependence of the inverse square scale parameter on the vortex-unbinding "Coulomb-gas" temperature  $\tau_\omega$ . The solid line is a fit according to Eq. (13).

ded by the periodic, quasiperiodic or fractal structure of the system creates new and interesting phenomena [3-13]. Since there are two competing periodicities, the physics of periodic arrays is somewhat similar to that of other modulated superconducting systems studied in the past [48, 49]. As the frustration  $f$  changes, the array is driven through a sequence of commensurate (C) ( $f = p/q$  rational, where  $p$  and  $q$  are integers such that  $p/q$  is an irreducible fraction) and incommensurate (I) ( $f$  irrational) vortex phases [17,30,38].

The complex oscillatory behaviour of the ac response  $\delta V_\omega(f)$  resulting from the drastic change in pinning occurring at a CI transition is shown in Fig. 6 for a proximity-effect array [7]. Prominent structures emerge in both the dissipative (a) and inductive (b) components of  $\delta V_\omega(f)$  in correspondence to C-vortex phases defined by  $f = p$ ,  $f = p/2$  and  $f = p/3$ . The origin of these structures as well as their evolution with temperature can be understood in terms of periodic vortex pinning and thermally activated defects. At low temperatures [ $T \ll T_c(f)$ ], where the influence of topological excitations is negligible, a C-phase is pinned by the periodic potential provided by the array. As a function of  $f = p/q$ , the critical current,  $i_c(f = p/q)$ , of the array, which is a measure of the pinning strength, has a strongly discontinuous upper bound  $\pi(e/\hbar)E(p/q)/q$ , where  $E(p/q)$  is the (non-monotonic) ground-state energy per junction [17,30]. In an I-phase the vortex lattice can slide freely, the upper bound for  $i_c(f)$  vanishing in the limit  $q \rightarrow \infty$ . As a consequence of the reduced vortex mobility due to pinning, there is a marked reduction in dissipation in a low-order (small  $q$ ) C-phase, a process resulting in the periodic sequence of dips one observes in the  $\text{Re}[\delta V_\omega(f)]$  signals of Fig. 6(a) at low temperatures. On the other hand, the commensurate peaks occurring in the inductive component of  $\delta V_\omega(f)$  [Fig. 6 (b)] reflect the lag in response enhanced by pinning in a low-order C-phase.

As the temperature rises and approaches  $T_c(f)$ , the low-temperature commensurate dips in  $\text{Re}[\delta V_\omega(f)]$  progressively transform into peaks which finally vanish above  $T_c(f)$  [Fig. 6(a)].

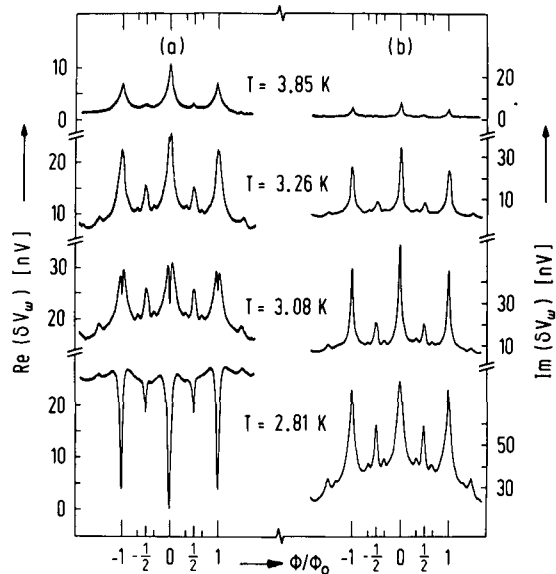


Fig. 6. Real (a) and imaginary (b) parts of the ac response at 4 kHz of a 2D array of proximity-effect Josephson junctions as a function of the frustration  $f = \Phi/\Phi_0$ .

Simultaneously, a rapid degradation of the commensurate peaks in  $\text{Im}[\delta V_\omega(f)]$  is observed in the critical region [Fig. 6(b)]. This evolution suggests the presence of thermally activated defects which, on account of their high mobility, generate additional dissipation and reduce the lag in response in a C-phase. For  $f = p \neq 0$  we have shown [7] that the dynamics of these defects has features allowing their identification as the vortex excitations of the KT theory. For a fully-frustrated array ( $f = p/2$ ) both vortex and domain-wall excitations are expected to be relevant for the critical behaviour of the system [1]. The ac response at 8.5 kHz and full frustration ( $f = 1/2$ ) of the Pb/Cu/Pb array studied in Sec. 3 is shown in Fig. 7 as a function of temperature. As expected [17,25,29], the transition, when compared to that

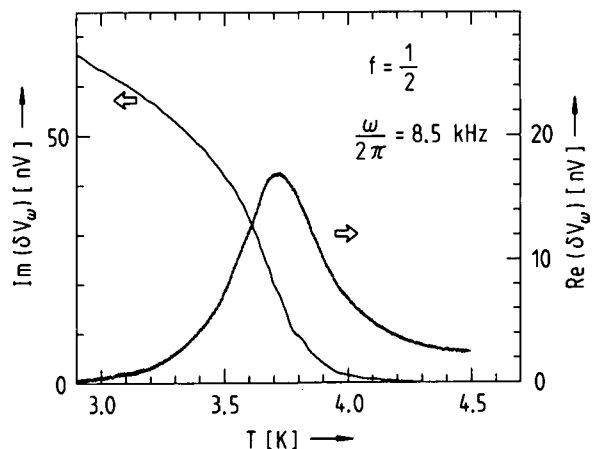


Fig. 7. Temperature dependence of the complex ac response of the proximity-effect array of Fig. 1 at full frustration ( $f = 1/2$ ).

at zero frustration (Fig. 1), occurs at a lower temperature. In terms of reduced critical temperatures we find  $T_c(0)/T_c(1/2) \approx 1.8$ , in good agreement with the ratio obtained from Monte Carlo calculations [ $T_c(0)/T_c(1/2) \approx 2$ ] [17]. The overall temperature dependence of both components of the response is not significantly different from that observed for the unfrustrated system. This tends to support the interpretation that vortex excitations play a major role in determining the critical behaviour of a fully frustrated array. However, in the absence of a detailed dynamical theory taking into account the influence of both vortices and domain walls, no definitive conclusions about the exact nature of the phase transition of a fully frustrated array can be drawn. This unsolved problem should deserve more study in the future.

#### ACKNOWLEDGMENTS

We would like to thank B. Jeanneret, R. Théron, D. Ariosa and A. Vallat for many useful discussions. This work was supported by the Swiss National Science Foundation.

#### REFERENCES

- 1) D.J. Resnick, J.C. Garland, J.T. Boyd, S. Shoemaker and R.S. Newrock: *Phys. Rev. Lett.* **47** (1981) 1542.
- 2) D.W. Abraham, C.J. Lobb, M. Tinkham and T.M. Klapwijk: *Phys. Rev. B* **26** (1982) 5268.
- 3) R.F. Voss and R.A. Webb: *Phys. Rev. B* **25** (1982) 3446.
- 4) R.A. Webb, R.F. Voss, G. Grinstein and P.M. Horn: *Phys. Rev. Lett.* **51** (1983) 690.
- 5) M. Tinkham, D.W. Abraham and C.J. Lobb: *Phys. Rev. B* **28** (1983) 6578.
- 6) D. Kimhi, F. Leyvraz and D. Ariosa: *Phys. Rev. B* **29** (1984) 1487.
- 7) Ch. Leemann, Ph. Lerch, G.A. Racine and P. Martinoli: *Phys. Rev. Lett.* **56** (1986) 1291.
- 8) R.K. Brown and J.C. Garland: *Phys. Rev. B* **33** (1986) 7827.
- 9) B.J. van Wees, H.S.J. van der Zant and J.E. Mooij: *Phys. Rev. B* **35** (1987) 7291.
- 10) B. Pannetier, J. Chaussy, R. Rammal and J.C. Villegier: *Phys. Rev. Lett.* **53** (1984) 1845.
- 11) J.M. Gordon, A.M. Goldman, J. Maps, D. Costello, R. Tiberio and B. Whitehead: *Phys. Rev. Lett.* **56** (1986) 2280.
- 12) A. Berhooz, M.J. Burns, H. Deckman, D. Levine, B. Whitehead and P.M. Chaikin: *Phys. Rev. Lett.* **57** (1986) 368.
- 13) K.N. Springer and D.J. Van Harlingen, preprint.
- 14) B. Jeanneret, Ch. Leemann and P. Martinoli: Contribution EM 17 in the Proceedings of this Conference.
- 15) C.J. Lobb, D.W. Abraham and M. Tinkham: *Phys. Rev. B* **27** (1983) 150.
- 16) C.J. Lobb: *Physica* **126B** (1984) 319.
- 17) S. Teitel and C. Jayaprakash: *Phys. Rev. B* **27** (1983) 598, and *Phys. Rev. Lett.* **51** (1983) 1999, and *J. Physique Lett.* **46** (1985) L33.
- 18) J.M. Kosterlitz and D.J. Thouless: *J. Phys. C* **6** (1973) 1181.
- 19) T. Ohta and D. Jasnow: *Phys. Rev. B* **20** (1979) 139.
- 20) M.Y. Choi and S. Doniach: *Phys. Rev. B* **31** (1985) 4516.
- 21) M. Yosefin and E. Domany: *Phys. Rev. B* **32** (1985) 1778.
- 22) M.Y. Choi and D. Stroud: *Phys. Rev. B* **32** (1985) 5773.
- 23) E. Granato and J.M. Kosterlitz: *Phys. Rev. B* **33** (1986) 4767.
- 24) E. Granato: *J. Phys. C* **20** (1987) L215.
- 25) W.Y. Shih and D. Stroud: *Phys. Rev. B* **28** (1983) 6575, and *Phys. Rev. B* **30** (1984) 6774, and *Phys. Rev. B* **32** (1985) 158.
- 26) S. Miyashita and H. Shiba: *J. Phys. Soc. Jpn.* **53** (1984) 1145.
- 27) D.H. Lee, J.D. Joannopoulos, J.W. Negele and D.P. Landau: *Phys. Rev. B* **33** (1986) 450.
- 28) B. Berge, H. T. Diep, A. Ghazali and P. Lallemand: *Phys. Rev. B* **34** (1986) 3177.
- 29) P. Minnhagen: *Phys. Rev. B* **32** (1985) 7548.
- 30) T.C. Halsey: *Phys. Rev. B* **31** (1985) 5728, and *J. Phys. C* **18** (1985) 2437.
- 31) V.S. Dotsenko and G.V. Uimin: *J. Phys. C* **18** (1985) 5019.
- 32) S.E. Korshunov and G.V. Uimin: *J. Stat. Phys.* **43** (1986) 1; S. E. Korshunov: *J. Stat. Phys.* **43** (1986) 17.
- 33) M. Cyrot: *Rep. Prog. Phys.* **36** (1973) 103.
- 34) D.E. Mc Cumber: *J. Appl. Phys.* **39** (1968) 3113.
- 35) M. Tinkham: *Introduction to Superconductivity* (McGraw Hill, New York, 1975) Chap. 6, p. 204.
- 36) A.F. Hebard and A.T. Fiory: *Phys. Rev. Lett.* **44** (1980) 291, and *Ordering in Two dimensions*, ed. S.K. Sinha (North Holland, New York, 1980) p. 181, and *Physica (Amsterdam)* **109** and **110B** (1982) 1637.
- 37) R. Côté and A. Griffin: *Phys. Rev. B* **34** (1986) 6240.
- 38) P. Martinoli, Ch. Leemann and Ph. Lerch: *Non-linearity in Condensed Matter*, ed. A.R. Bishop, D.K. Campell, P. Kumar and S.E. Trullinger (Springer Series in Solid-State Sciences, Berlin, 1987) Vol. 69, p. 361.
- 39) V. Ambegaokar, B.I. Halperin, D.R. Nelson and E.D. Siggia: *Phys. Rev. B* **21** (1980) 1806.
- 40) B.I. Halperin and D.R. Nelson: *J. Low Temp. Phys.* **36** (1979) 599.
- 41) S.R. Shenoy: *J. Phys. C* **18** (1985) 5163.
- 42) J.M. Kosterlitz: *J. Phys. C* **7** (1974) 1046.
- 43) J.E. Mooij: *Percolation Localization and Superconductivity*, ed. A.M. Goldman and S.A. Wolf (Plenum Press, New York, 1984) NATO ASI SERIES Vol. B109, p. 325.
- 44) A.M. Kadin, K. Epstein and A.M. Goldman: *Phys. Rev. B* **27** (1983) 6691.
- 45) P.W. Adams and W.I. Glaberson: *Phys. Rev. B* **35** (1987) 4633.
- 46) S. Alexander: *Phys. Rev. B* **27** (1983) 1541, and *J. Physique* **44** (1983) 805.
- 47) R. Rammal, T.C. Lubensky and G. Toulouse: *Phys. Rev. B* **27** (1983) 2820.
- 48) D. Daldini, P. Martinoli, J.L. Olsen and G. Berner: *Phys. Rev. Lett.* **32** (1974) 218.
- 49) A.T. Fiory, A.F. Hebard and S. Somekh: *Appl. Phys. Lett.* **32** (1978) 73.